Design of unpaved roads and trafficked areas with geogrids

J. P. Giroud, *GeoServices Consulting Engineers*, C. Ah-Line, *Woodward-Clyde Consultants*, and R. Bonaparte, *The Tensar Corporation*

An increasing number of unpaved roads and trafficked areas, such as parking lots and drilling pads, are built using geogrids. These unpaved structures are composed of a base layer placed on a subgrade soil and reinforced with one or several layers of geogrids. At the present time, no design method for these structures is available. This paper presents the initial development of a design method for geogrid-reinforced unpaved structures. The paper begins by reviewing the mechanisms through which geogrids can improve the performance of an unpaved structure. An analysis of published full-scale unpaved road test data is presented next. The analytical development of the design method is then described, as is the preparation of design charts. The charts give base layer thickness as a function of the subgrade soil undrained shear strength, geogrid tensile stiffness, traffic, and allowable rut depth of the unpaved structure. The use of the charts is illustrated by a design example. It is pointed out that the design method is still undergoing development and that field and/or laboratory verification of the method is required. When fully developed, the method will allow designers to evaluate the cost effectiveness of geogrids as compared with other methods for constructing unpaved roads and trafficked areas.

INTRODUCTION

Geogrids (Fig. 1) are increasingly used to reinforce geotechnical structures, including unpaved roads and trafficked areas. Unpaved roads and trafficked areas ("unpaved structures"), consisting of a base layer (usually made of aggregate) placed on a subgrade soil, can be reinforced by geogrids placed within the base layer and/or, more often, at the base layer/subgrade interface. Such reinforcement improves the performance of the structure: for a given base layer thickness and a given allowable rut depth, the traffic can be increased, in comparison with the allowable traffic on the same thickness of unreinforced base layer; or, for a given base layer thickness and a given traffic, the rut depth is smaller than with an unreinforced base layer. Alternatively, for the same traffic and allowable rut depth, the use of geogrid reinforcement allows: a reduction in base layer thickness in comparison with the thickness required when the base layer is unreinforced; or construction of a base layer with material of lesser quality than usually required.

The improved unpaved structure performance associated with geogrid usage was recognized by first users. At present, however, no design method specifically developed for geogrid-reinforced unpaved structures is available. Design methods developed for geotextile-reinforced unpaved structures are not suitable because they do not take into account the mechanism of geogrid/base layer material interlocking. However, certain other mechanisms by which geogrids and geotextiles reinforce unpaved structures are similar, and consequently design methods for geogrid-reinforced unpaved structures may utilize features from existing geotextile design methods.

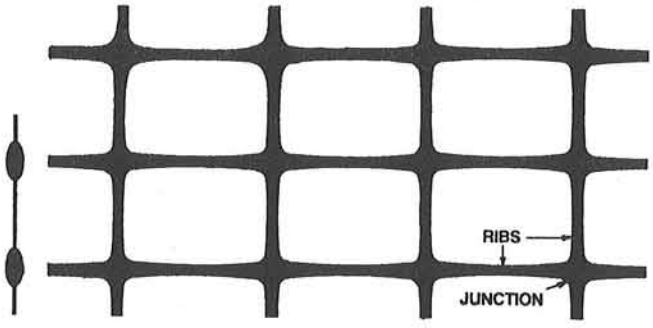

Fig. 1 Typical geogrid used in unpaved structures.

Starting from the design method published by Giroud and Noiray (1981) for geotextile-reinforced unpaved roads, a design method for geogrid-reinforced unpaved structures is currently being developed. This paper presents the initial analytical development of the method based on the authors' understanding of the behavior of unreinforced and reinforced unpaved structures. A preliminary design chart is presented with a design example. The design method is discussed and recommendations for additional work are presented .

CONCEPT AND BEHAVIOR OF UNPAVED STRUCTURES

Concept of Unpaved Structure

When a given traffic cannot be supported by a soil ("subgrade soil") because of insufficient bearing capacity, the traffic load should be distributed so that the stress on the subgrade soil becomes less than the subgrade soil bearing capacity. In unpaved structures, load distribution can be achieved by placing a layer of material ("base layer") between the load and the subgrade soil.

To achieve its load distribution function, the base layer should have: (i) adequate mechanical properties; and (ii) sufficient thickness.

To maintain its load distribution function under repeated loading, the base layer must remain intact, requiring that: (i) deformations of the subgrade soil be limited to prevent lateral or vertical displacements at the bottom of the base layer; and (ii) the mechanical properties of the base layer be such that it is not sheared or degraded by traffic loads.

In comparison to paved structures where only small deformations can be accepted, rather large deformations are often acceptable in unpaved structures. This is the case with construction site access roads where earthwork equipment is available to maintain the base layer (fill ruts and regrade). Since failure mechanisms and magnitude of deformations for paved and unpaved roads are usually different, it is not recommended that methods developed for paved structures be used to design unpaved structures and vice versa. For instance, using unpaved road design methods to evaluate the effect of geotextiles or geogrids in paved roads is inadequate.

Polymer grid reinforcement. Thomas Telford Limited, London, 1985

Performance of an Unreinforced Unpaved Structure

The performance of an unreinforced unpaved structure is considered satisfactory until failure occurs. A road or trafficked area is considered failed when surface deformations are such that conditions for traffic become unacceptable. (The criterion usually considered is the rut depth, defined subsequently.) Unacceptable deformations can occur after one axle passage if the axle load exceeds the bearing capacity of the structure. Unacceptable deformations can also occur after several passages, as a result of:

- o accumulation of small permanent deformations occuring at each axle passage and accelerated by progressive deterioration of the structure; and/or
- o large deformation associated with shear failure of the structure which occurs when the bearing capacity becomes smaller than the axle load as a result of progressive deterioration of the structure.

Deterioration of the structure results from deterioration of the subgrade and deterioration of the base layer. Progressive deterioration of the subgrade results from the decrease of shear strength of the subgrade soil due to fatigue generated by repeated loading. Progressive deterioration of the base layer occurs through one or a combination of the following mechanisms affecting its thickness and/or mechanical properties:

- o lateral displacement of base layer material resulting from tensile and shear strains related to bending and low confining stresses at the bottom of the base layer;
- o contamination of base layer by fine particles moving upward from subgrade;
- o sinking of base layer aggregate into subgrade soil; and
- o breakdown of base layer aggregate due to repeated loading and abrasion.

Progressive deterioration of the structure has three consequences:

- o acceleration of the occurence of unacceptable surface deformations resulting from accumulation of small permanent deformations;
- o decreased shear strength of both base layer material and subgrade soil and increased risk of shear failure; and
- o decreased ability of the base layer to distribute loads (because of thickness reduction and decrease in mechanical properties of the base layer), resulting in increased applied stress to the subgrade.

Behavior of a Reinforced Unpaved Structure

Since failure of an unpaved structure results from base layer and/or subgrade failure, either or both should be prevented or delayed to improve the performance of the structure. Geogrids can be placed at the base layer/subgrade interface or at various levels within the base layer. They can improve performance and prevent or delay progressive deterioration of the unpaved structure as discussed below.

Influence of a Geogrid on Base Layer Behavior

Geogrids can improve the performance of the base layer as a result of interlocking between geogrid and base layer material (especially if this material is aggregate). By interlocking with the base layer aggregate, geogrids provide reinforcement which can prevent shear failure and reduce permanent deformations of the base layer. According to McGown and Andrawes (1977), optimum reinforcement depth is approximately 0.3 times the width of the load. Raymond and Hayden (1983) found the optimum depth to be in the range of 0.3 to 0.6 times the load width. The width of a typical dual wheel contact area is approximately 0.3m (as discussed later in this paper). Consequently, the optimum depth of geogrid would be of the order of 0.1m to 0.2m. It is also important to consider any possible detrimental effects of reinforcement on the behavior of base layers. For instance, it is known that a smooth slippery surface at a depth smaller than the width of the load decreases the shear strength of the base layer. This would be the case of a smooth surface geotextile placed at a depth less than approximately 0.3m under a typical dual wheel. Geogrids do not act as slip surfaces because of their interlocking with aggregate, and, therefore, the considered detrimental effect is not relevant.

Geogrids can prevent or delay progressive deterioration of the base layer (i.e., base layer thickness reduction and decrease in base layer material properties) as a result of interlocking between geogrid and base layer material. The influence of geogrids on the actions leading to progressive deterioration of the base layer aggregate is discussed below:

- o Lateral Displacement of Base Layer Aggregate. - By interlocking with the base layer aggregate, geogrids reduce permanent lateral displacements which accumulate with increasing numbers of load repetitions. Optimum placement of the geogrid is as described above. Reduced displacements result in reduced deterioration of base layer material properties while preserving the effective thickness of the base layer.
- o Contamination. - By interlocking with the base layer aggregate, a geogrid, placed at the bottom of the base layer, prevents lateral movements of aggregate, thus preventing development of openings at the bottom of the base layer and limiting the rapidity and extent of penetration of fine subgrade soil particles into the aggregate. The effectiveness of geogrids in limiting contamination of base layer material by fine soil particles depends on several parameters including : subgrade soil consistency, water content and shear strength; and, particle size distribution of aggregate.
- o Aggregate Sinking. - By interlocking with the base layer aggregate, a geogrid prevents aggregate stones from sinking into the subgrade soil. Experience indicates that aggregate sinking is minimized through use of well-graded materials with maximum particle size at least one-half the width of the grid aperture.
- o Aggregate Breakdown. - By interlocking with the base layer aggregate and reducing movements, geogrids can decrease the amount of aggregate breakdown. This is particularly important when weak aggregate is used.

Influence of Geogrids on Subgrade Soil Behavior

Geogrids can improve performance of the subgrade soil in a way that is different from the way they improve the performance of the base layer. Unlike the base layer, subgrade soil properties cannot be improved or maintained through reinforcement. The performance of the subgrade can be improved only through changes in the boundary conditions, i.e., applied stresses and deformations. Geogrids can improve the performance of the subgrade soil through three mechanisms: confinement (which reduces deformations); and improved load distribution through the base layer and tensioned membrane effect (which reduces stresses).

- Confinement. - When the vertical stress on the subgrade soil of an unreinforced unpaved structure exceeds the elastic limit (assuming elasto-plastic behavior), local shear failure and large deformations ensue. These large deformations result in accelerated deterioration of the base layer and fatigue of the subgrade soil, causing the subgrade soil to be subjected to ever higher stress levels (i.e., an increasing ratio between applied and allowable stress). Consequently, after a relatively small number of vehicle passages the plastic limit (ultimate bearing capacity) of the subgrade soil is exceeded and general shear failure occurs. Experience has shown that if the subgrade soil is confined, deformations resulting from local shear failure do not become large and the subgrade soil can support a vertical stress close to its plastic limit (which is significantly higher that its elastic limit). Confinement requires continuity of the reinforcing element. Geotextiles provide confinement because they have small openings. Geogrids provide confinement if the quantity of subgrade soil escaping through geogrid openings is not sufficient to cause heave of the base layer.

- Load Distribution. - As explained previously, load distribution results from the mechanical properties and thickness of the base layer. Geotextiles, by separating base layer and subgrade soil, prevent aggregate contamination and aggregate sinking. Separation, therefore, reduces degradation of the mechanical properties of the aggregate and helps maintain the thickness of the base layer. However, as the unpaved road structure deforms, the base layer aggregate spreads laterally. Due to the absence of interlocking, a geotextile placed at the base layer/subgrade interface, does little to prevent lateral displacement of the base layer aggregate. In contrast, a geogrid is expected to reduce lateral displacement due to interlocking with aggregate. Also, the geogrid tensile stiffness adds to the stiffness of the base layer. The result is a stiffer base layer with reduced deterioration. The base layer is therefore able to provide better applied load distribution than possible with unreinforced, or geotextile-reinforced, base layers.

- Tensioned Membrane Effect. - If the subgrade soil is incompressible (such as saturated clay), deformation of the subgrade soil under the wheels causes heave between and beyond the wheels. Therefore, the geogrid exhibits a wavy shape; consequently, it is stretched. When a stretched flexible material has a curved shape, normal stress against its concave face is higher than normal stress against its convex face. This is known as the "tensioned membrane effect". Therefore: (i) between the wheels and to a lesser extent beyond the wheels, the normal stress applied by the geogrid on the subgrade is higher than the normal stress applied by the base layer on the geogrid; and (ii) under the wheels, the normal stress applied by the geogrid on the subgrade is smaller than the normal stress applied by the wheels plus the base layer on the geogrid. This action provides two beneficial effects, confinement of the subgrade soil between and beyond the wheels (as discussed above), and reduction of the stress applied by the wheels on the subgrade. The stress reduction resulting from the tensioned membrane effect is effective if traffic loads are repeated at exactly the same location (i.e., if the traffic is channelized), and if the tensile stress in the reinforcement does not decrease with time (i.e., if the reinforcement has low creep susceptibility at working loads).

Geogrids can reduce subgrade soil deterioration by reducing the magnitude of repeated deformation of the structure, thereby reducing disturbance of the subgrade soil and, consequently, fatigue resulting in a progressive decrease in shear strength of the subgrade soil.

DESIGN PARAMETERS

Geometry of Unpaved Structure

The thickness of base layer is termed h_o when there is no reinforcement and h when there is reinforcement. The subscript s is affixed to h_o and h when the axle load is the standard axle load (defined subsequently). The ratio, R, between h and h_o for a same axle load is called the thickness ratio. If there is only one geogrid, it is assumed to be at the base layer/subgrade interface. If there are two geogrids, it is assumed that one is at the base layer/subgrade interface and that the other is in the base layer; the exact location of this second geogrid is not specified because this parameter is not considered in the method presented hereafter. The optimum depth of the second geogrid layer may be obtained from the previous discussion on the behavior of reinforced unpaved structures. The subgrade soil is assumed to be homogeneous, at least over a thickness, H, sufficient to allow development of subgrade soil failure. The thickness H can be estimated using a classical bearing capacity analysis which shows that H is usually less than 1.5m. Therefore, the assumption of homogeneous subgrade soil is often valid.

Traffic

Traffic can be channelized, as is the case on a road, or unrestricted over an area. A channelized traffic is characterized by the number of passages, N, of a given axle during the design life of the structure. A traffic unrestricted over an area is less easy to characterize and some judgement on the designer's part is required. However, in most trafficked areas there are locations, such as entrances and exits, where traffic is channelized and can therefore be characterized by a number of passages.

Axles and Loads

The geometry of axle is depicted in Fig. 2a in which e is the distance between the midpoints of the two sets of wheels. Dual wheels are considered because they are more common than single wheels for trucks using unpaved structures.

The axle load, P, is considered to be evenly distributed between the four wheels:

$$P = 4A_c p_c \qquad (1)$$

where: P = axle load (N); A_c = contact area of a tire (m^2); and p_c = tire inflation pressure (N/m^2), assumed to be equal to the average value of the actual contact pressure (non-uniformly distributed) between each tire and the base layer.

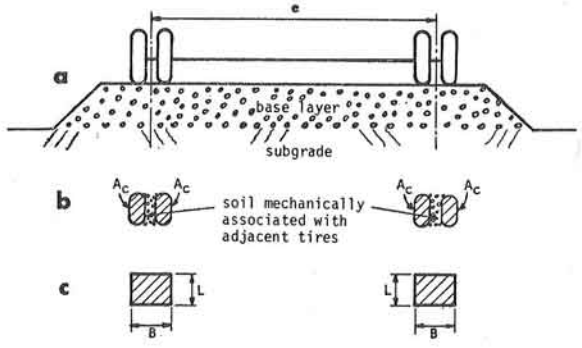

Fig. 2 Vehicle axle and contact area: (a) Geometry of vehicle axle with dual wheels; (b) Tire contact areas; and (c) Equivalent contact area used in analysis.

The soil between the tires of a dual wheel is mechanically associated with these tires (Fig. 2b). Since no failure of the base layer material and subgrade soil is expected to occur between the tires, each double contact area $2A_c$ is replaced in the theoretical study by a rectangle L x B of larger area (Fig. 2c). By examining several dual tire prints, the following value appears reasonable:

$$LB = 2A_c\sqrt{2} \quad (2)$$

The actual contact pressure (nonuniformly distributed) between each tire and the base layer induces the same mechanical effects in the subgrade soil as an "equivalent contact pressure", p_{ec}, (assumed uniformly distributed) between the rectangle L x B and the base layer; therefore:

$$P = 2LBp_{ec} \quad (3)$$

The relationship between the equivalent contact pressure, p_{ec}, and the tire inflation pressure, p_c, is deduced from Eqs. 1, 2, and 3:

$$p_{ec} = p_c/\sqrt{2} \quad (4)$$

Examination of typical dual tire prints leads to the following approximate value for the length L, in the case of on-highway trucks:

$$L = B/\sqrt{2} \quad (5)$$

Eliminating L from Eqs. 3 and 5 and using Eq. 4 yield:

$$B = \sqrt{P/p_c} \quad (6)$$

Eq. 6 is useful for the subsequent analysis because vehicles are usually characterized by axle load, P, and tire inflation pressure, p_c, which is almost equal to the actual contact pressure as previously stated. For the American-British standard axle load ($P = P_S = 80$ kN) and a tire inflation pressure of 620 kN/m^2, L = 0.25m and B = 0.36m.

Different relationships would be necessary for other types of trucks such as off-highway trucks, and construction equipment.

Also, replacement of the actual contact area by the rectangle LxB is valid only for analyzing effects on the subgrade (the only failure mechanism explicitly considered in the proposed design method). It may not be appropriate for evaluating shear failure of the base layer.

Rut Depth

When the traffic is channelized, ruts develop at the surface of the base layer. The rut depth, r, is the vertical distance between the highest point of the base layer surface between the wheels and the lowest point of the rut. In the case of trafficked areas, where the traffic is not channelized, an erratic pattern of ruts develop. The rut depth can then be defined as the vertical distance between high spots and low spots of the base layer surface in the considered area.

Properties of Base Layer

In this study, the base layer consists of an aggregate which is assumed to have the properties usually required to ensure adequate distribution of the applied load. In a practical sense, this means that the California Bearing Ratio (CBR) of the aggregate is larger than 80.

No other base layer material (such as sand, silt, etc.) is considered in this study.

Properties of Subgrade Soil

The subgrade soil is assumed to be saturated and to have a low permeability (silt, clay). Therefore, under quick loading (such as traffic loading), the subgrade soil behaves in an undrained manner. Practically, this means that the subgrade soil is incompressible and frictionless. Consequently its shear strength is equal to its undrained cohesion, c_u.

The value of c_u is measured in the laboratory using unconsolidated undrained or unconfined triaxial tests, or quick direct shear tests; and in the field using vane shear test. The value of c_u can also be approximated using a cone penetrometer or deduced from CBR value (less than 5) using one of the following relationships:

$$c_u = q_c/10 \quad (7)$$

$$c_u\ (N/m^2) = 30\,000\ CBR \quad (8)$$

where: q_c = cone resistance (N/m^2); and CBR = California Bearing Ratio (dimensionless). Equations 7 and 8 should be replaced by site-specific strength correlations where available.

Properties of Geogrids

The geogrid mechanical properties relevant to this study are described by the geogrid behavior in a uniaxial tensile test giving the force per unit width, F/w, as a function of the elongation, ε.

Force per unit width-elongation curves related to the longitudinal and the transverse direction of the geogrid Tensar SS2 are presented in Fig. 3. The definition of the secant tensile stiffness, K, is shown on one of these curves.

The curves presented in Fig. 3 have been obtained for a rate of elongation of 25% per minute, at 20°C. This rate of elongation corresponds approximately to the quick loading by a moving vehicle. Values of the tensile stiffness obtained for a 2% elongation are 400 kN/m for the longitudinal direction and 700 kN/m for the transverse direction. An average value of 500

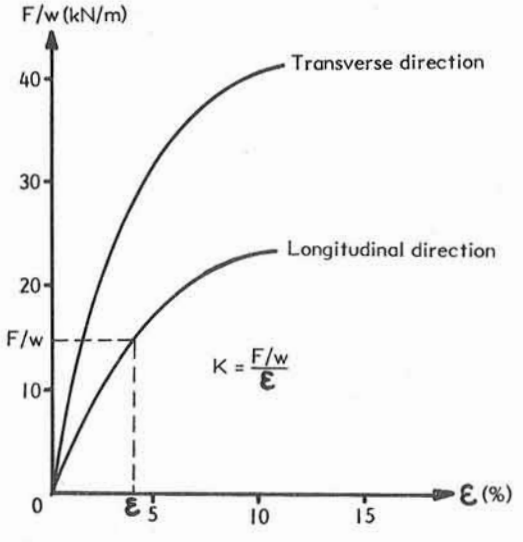

Fig. 3 Typical force per unit width - elongation curve of geogrid. K is the secant tensile stiffness of the geogrid at elongation ε.

kN/m has been considered in the development of the design method. The average value for the tensile stiffness of the geogrid Tensar SS1 is estimated at 300 kN/m, based on limited test data.

The tensile behavior of polymeric material depends on the rate of elongation. Smaller values of tensile stiffness and tensile strength, and larger values of elongation at failure would be obtained for lower rates of elongation.

In addition to the tensile behavior, it is necessary to address the friction characteristics of the geogrid/base layer aggregate interface. The limited available data leads to the conclusion that for the types of geogrids and base layer aggregate considered herein, the frictional resistance at the geogrid/base layer aggregate interface is approximately equal to the frictional resistance of the base layer aggregate alone. Thus, geogrids, through their interlocking with the base layer material, have adequate friction characteristics to prevent failure by sliding along the geogrid/base layer interface.

DESIGN OF UNREINFORCED UNPAVED STRUCTURES

The proposed method for designing geogrid-reinforced unpaved structures has been established using the design of unreinforced unpaved structures as a starting point.

Test Results on Unreinforced Unpaved Roads

An extensive test program on unreinforced unpaved roads has been conducted by the Corps of Engineers (Hammit, 1970). The failure criterion for this study was a rut depth of 0.075 m. From the test results, Webster and Alford (1978) established a chart giving the thickness of the base layer as a function of the number of passages, N, and the CBR of the subgrade soil for a standard axle load, P_S = 80 kN. Giroud and Noiray (1981) found the following formula to be in good agreement with Webster and Alford's chart:

$$h_{os} = 0.19 \log N / (CBR)^{0.63} \quad (9)$$

where: h_{os} = base layer thickness (subscript o refers to unreinforced and s to standard axle) (m); N = number of passages of standard axle (load P_S = 80 kN); and CBR = California Bearing Ratio of subgrade soil. The use of Eq. 9 is restricted to standard axle load and 0.075 m rut depth.

Combining Eqs. 8 and 9 yields:

$$h_{os} = 125 \log N / c_u^{0.63} \quad (10)$$

where: c_u = undrained shear strength (cohesion) of the subgrade soil (h_{os} in m and c_u in N/m^2 exclusively).

To extend Eq. 10 to rut depths r other than 0.075 m, Giroud and Noiray have proposed replacing log N by $[\log N - 2.34 (r - 0.075)]$. This expression has been empirically deduced from test results presented by Webster and Watkins (1977), showing that the increase of rut depth with number of passages is much more marked as soon as the rut depth exceeds 0.075 m. Eq. 10 thus becomes:

$$h_{os} = \left[125 \log N - 294 (r-0.075)\right] / c_u^{0.63} \quad (11)$$

(h_{os} and r in m and c_u in N/m^2 exclusively)

This equation has been established by extrapolation and should not be used when the number of passages exceeds 10 000.

A chart for the design of unreinforced unpaved roads, established using Eq. 11 is presented in Fig. 4.

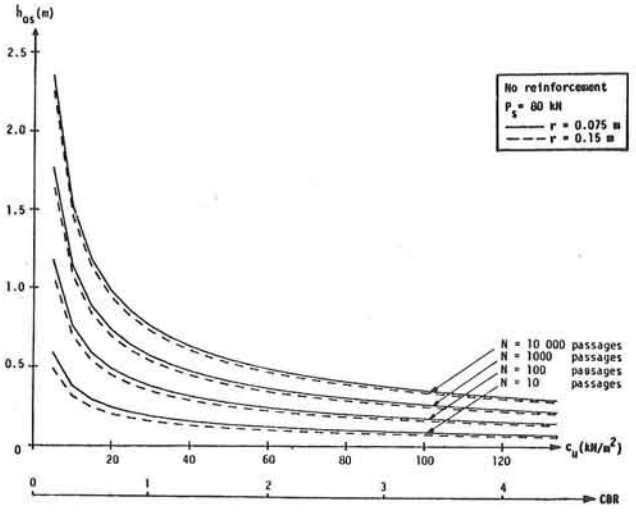

Fig. 4 Unreinforced base layer thickness, h_{os}, versus subgrade soil shear strength, c_u, for a standard axle load (P_S = 80kN) and two values of rut depth r.

Interpretation of Test Results on Unreinforced Unpaved Roads

As explained earlier in this paper, progressive deterioration of the subgrade soil and the base layer are major factors leading to the failure of unpaved roads. Therefore, it is important to identify the relative influence of these two mechanisms in the above mentioned test data.

Progressive Deterioration of the Subgrade Soil

The mechanical property which governs the behavior of the subgrade soil is its undrained shear strength. Therefore, the progressive deterioration of the subgrade soil can be expressed by a decrease of its undrained shear strength when the number of passages increases:

$$c_{uN} = \lambda c_u \quad (12)$$

where: c_{uN} = undrained shear strength (cohesion) of the subgrade soil at the Nth passage of the axle (N/m^2); and c_u = undrained shear strength of the subgrade soil before or at the first passage of the axle (N/m^2).

The coefficient λ represents the progressive deterioration or fatigue of the subgrade soil generated by repeated loading due to traffic. The following conditions should be met by λ :

$\lambda = 1$ if N = 1 ($c_{uN} = c_u$)

$\lambda = 1$ if $c_u = 0$ (a liquid is not susceptible to fatigue)

$\lambda < 1$ if $c_u > 0$ and $N > 1$ ($c_{uN} < c_u$)

These conditions can be met using various empirical equations, including:

$$\lambda = c_{uN}/c_u = 1/\left[1 + (\log N)^{3/2} c_u/1000\right] \quad (13)$$

(with c_u in kN/m^2 exclusively)

Values of λ calculated with Eq. 13 are presented in Fig. 5.

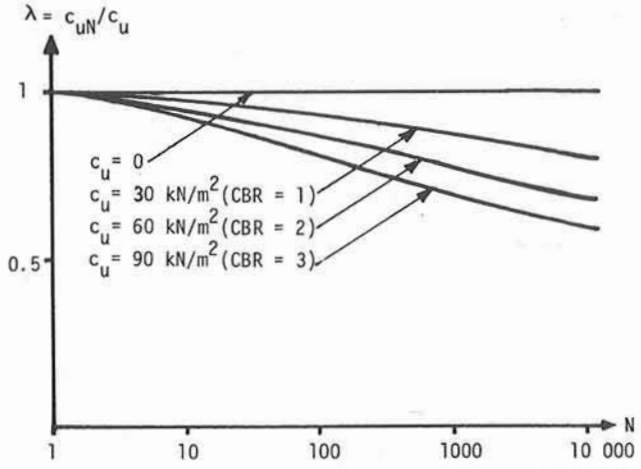

Fig. 5 Coefficient of fatigue, λ, of the subgrade soil versus number of passages, N, calculated using Eq. 13.

Progressive Deterioration of the Base Layer

Failure of the subgrade soil occurs where applied stresses exceed the bearing capacity of the subgrade soil. As discussed earlier in this paper, progressive deterioration of the base layer gradually increases stresses on the subgrade soil. These stresses could be estimated using linear or nonlinear elastic or elasto-plastic analyses. Such analyses would necessitate detailed numerical calculations. A simpler approach, used herein, consists of assuming that the base layer provides a pyramidal distribution of the applied wheel loads (Fig. 6). The pyramidal distribution is a classic assumption in soil mechanics as discussed by Giroud (1982), and is suitable for the comparison of peak vertical stress magnitudes, as used herein. The vertical stress, p_{os}, on the subgrade, calculated using the pyramidal distribution, is:

$$p_{os} = (P_s/2)/\left[(B+2\,h_{os}\tan\alpha_o)(L+2\,h_{os}\tan\alpha_o)\right]+\gamma h_{os} \qquad (14)$$

where: P_s = standard axle load (80 kN); $P_s/2$ = dual-wheel load (40 kN); B and L = width and length respectively of the rectangular area replacing the actual contact area between a dual wheel and the surface of the base layer (m); h_{os} = base layer thickness (m); α_o = load distribution angle for unreinforced base layer; γ = unit weight of soil (N/m^3); and γh_{os} = gravity stress at depth h_{os} (i.e., at the bottom of the base layer) (N/m^2) (Note: subscript o refers to unreinforced and subscript s to standard axle).

In Eq. 14, it is assumed that the axle is long enough that the pyramids related to the two dual wheels do not interfere. This assumption is valid for most values of α_o and h_{os} typically considered.

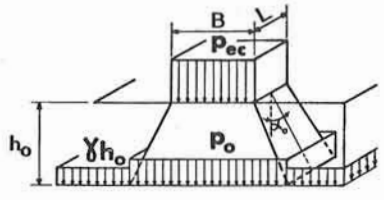

Fig. 6 Concept of pyramidal load distribution.

Progressive deterioration of the base layer may be modeled by a decrease of load distribution angle and/or effective base layer thickness when the number of passages increases. A decrease in the load distribution angle is considered in this study and is used to evaluate the progressive increase of applied subgrade stress due to base layer deterioration. To evaluate the assumed decrease of this parameter in the test data presented in the previous section, the value of p_{os} obtained using Eq. 14 should be compared with the maximum stress that can be allowed on the subgrade soil.

As discussed previously for unreinforced unpaved roads, the deformation of the surface of the subgrade soil, and therefore the rut depth, becomes large if the vertical stress on the subgrade soil exceeds the elastic limit, given by:

$$p_e = \pi c_{uN} + \gamma h_{os} \qquad (15)$$

where: c_{uN} = undrained shear strength (cohesion) of the subgrade soil at the Nth passage of the axle (N/m^2); and γh_{os} = gravity stress at depth h_{os} (i.e., at the bottom of the base layer) (N/m^2).

Combining Eqs. 14 and 15 yields:

$$\lambda c_u = c_{uN} = (P_s/2)/\left[\pi(B+2h_{os}\tan\alpha_o)(L+2h_{os}\tan\alpha_o)\right] \qquad (16)$$

where: $\lambda = c_{uN}/c_u$ = ratio between undrained shear strength of subgrade soil at the Nth passage and at the first passage.

The load distribution angle, α_o, can be calculated by combining Eqs. 5, 6, 9, 13 and 16, and solving the resulting quadratic equation:

$$\tan\alpha_o = \frac{\sqrt{(\sqrt{2}-1)^2 P_s/(2p_c)+2P_s/(\lambda\pi c_u)} - (\sqrt{2}+1)\sqrt{P_s/(2p_c)}}{6.5\log N/c_u^{0.63}} \qquad (17)$$

where: P_s = standard axle load (80 kN); p_c = tire inflation pressure (kN/m^2); and c_u = undrained shear strength (cohesion) of the subgrade soil (kN/m^2).

Values of $\tan\alpha_o$ calculated using Eq. 17, with a tire inflation pressure p_c = 620 kN/m^2, are presented in Fig. 7 which shows that $\tan\alpha_o$ decreases as the number of passages increases. This illustrates that the ability of the base layer to distribute

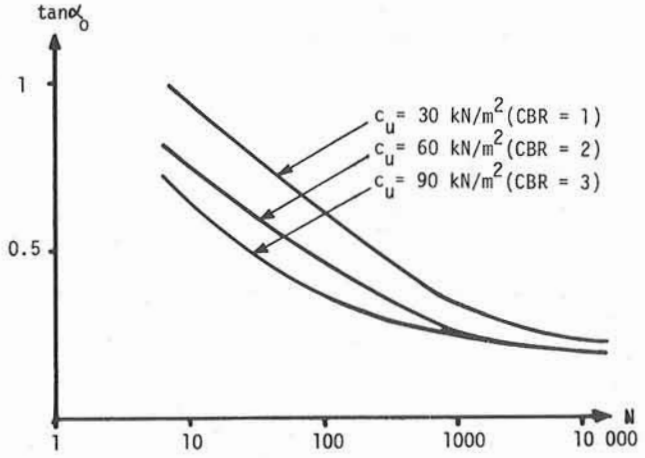

Fig. 7 Load distribution angle, $\tan\alpha_o$, versus number of pasages, N, calculated using Eq. 17.

load decreases as the base layer progressively deteriorates due to repeated loading. This effect is more marked when the shear strength of the subgrade soil is smaller.

Although Eq. 13 is arbitrary, it is qualitatively valid because it meets the conditions for representing the progressive deterioration of the subgrade shear strength as explained above. Trends derived from Eq. 13 and shown in Fig. 5 and 7 can therefore be considered to qualitatively represent real behavior. These trends can be summarized as follows:

- Traffic causes progressive deterioration of the subgrade soil, expressed as a decrease of the subgrade soil shear strength when the number of passages increases. This deterioration is more marked for subgrade soils with a higher strength (Fig. 5).
- Traffic causes progressive deterioration of the base layer. This deterioration is more marked when the subgrade soil is softer (Fig. 7) because the softer the subgrade soil, the larger the magnitude and/or rate of action of the mechanisms for progressive deterioration cited previously (lateral displacement of base layer aggregate, contamination by fine subgrade soil, sinking of aggregate into subgrade soil, and breakdown of aggregate particles).

These findings, resulting from a theoretical interpretation of full scale tests, are in good agreement with generally accepted modes of failure in roads. From an immediate and practical view point, the above discussion provides the understanding and equations necessary to extend the design method for unreinforced unpaved structures with standard axle loads to unreinforced unpaved structures with any axle load and, more importantly, to the case of geogrid-reinforced unpaved structures.

Design of Unreinforced Unpaved Structures for Any Axle Load

Eqs. 10 and 11, established from test data, are valid only for standard axle loads (i.e., P_S = 80 kN). However, similar equations can be derived for other axle loads using Eq. 16, if it is assumed that base layer and subgrade behave in a similar manner as in the above discussed full scale tests, and that this behavior is dependent on the subgrade stress level.

Eq. 16 can be written for any axle load P, corresponding to a thickness h_o, by replacing P_S and h_{OS} by P and h_o, respectively. Combining the two versions of Eq. 16 and solving the resulting quadratic equation leads to:

$$h_o = \frac{\sqrt{(B-L)^2+4(B+2h_{OS}\tan\alpha_o)(L+2h_{OS}\tan\alpha_o)(P/P_S)}-(B+L)}{4\tan\alpha_o} \qquad (18)$$

where: h_o = base layer thickness corresponding to an axle load P (m); h_{OS} = base layer thickness corresponding to the standard axle load P_S = 80 kN (m); α_o = load distribution angle for unreinforced base layer; and B and L = width and length respectively of the rectangular area replacing the actual contact area between a dual wheel and the surface of the base layer (m). (Note: for P = P_S, it is easy to verify that Eq. 18 gives $h_o = h_{OS}$.)

Replacing h_{OS} in Eq. 18 by its value given in Eq. 10 or 11 enables one to determine the thickness of an unreinforced unpaved base layer, h_o, corresponding to any axle load P, and to prepare charts valid for any axle load similar to the charts presented in Fig. 4 for a standard axle load. Eq. 18 is valid only if the wheel print (represented by the rectangle B x L) is the same, or approximately the same, for the considered axle and the standard axle. A more complex equation would be necessary if the geometry of the two dual wheels were significantly different.

DEVELOPMENT OF A DESIGN METHOD FOR GEOGRID REINFORCED UNPAVED STRUCTURES

A discussion of the mechanisms through which a geogrid can improve the behavior of an unpaved structure has been presented earlier in this paper. The design method presented hereafter takes into account only three mechanisms: confinement of the subgrade soil, improved load distribution and tensioned membrane effect.

Influence of Confinement of the Subgrade Soil

As discussed previously, the vertical stress on the subgrade soil can be as large as the ultimate bearing capacity of the soil when confinement is provided. The ultimate bearing capacity (i.e., plastic limit) of the subgrade soil is expressed by:

$$p_{lim} = (\pi+2)\, c_{uN} + \gamma h \qquad (19)$$

where: c_{uN} = undrained shear strength (cohesion) of the subgrade soil at the Nth passage of the axle (N/m^2); and γh = gravity stress at depth h (i.e., at the bottom of the base layer) (N/m^2).

A comparison between Eqs. 15 and 19 outlines the benefit resulting from subgrade soil confinement by a geogrid; the term πc_{uN} in Eq. 15 referring to elastic limit (local shear) is replaced in Eq. 19 by the term $(\pi + 2)c_{uN}$ referring to plastic limit (general shear).

It has been assumed that the value of the undrained shear strength, c_{uN}, at the Nth passage for the confined subgrade is the same as for the unconfined subgrade, if the ratio between confined and unconfined subgrade stress is equal to the ratio between the plastic and elastic limit of the subgrade soil. The rationale behind this assumption is that fatigue of subgrade soil results from remolding caused by repeated deformations; and since deformations are of equivalent magnitudes in an unconfined soil at the elastic limit and a confined soil at the plastic limit, fatigue will be the same in both cases.

Influence of Load Distribution

The improvement in load distribution capability of the reinforced base layer relative to the unreinforced base layer can be quantified by replacing the angle α_o used in Eq. 14 by a larger angle α. The vertical stress transmitted by the base layer to the upper face of the geogrid becomes:

$$p' = (P/2)/\left[(B+2h\tan\alpha)(L+2h\tan\alpha)\right]+\gamma h \qquad (20)$$

where: P = axle load (N); P/2 = dual-wheel load (N); B and L = width and length respectively of the rectangular area replacing the actual contact area between a dual wheel and the surface of the base layer (m); h = base layer thickness (m); α = load distribution angle for reinforced base layer; γ = unit weight of soil (N/m^3); and γh = gravity stress at depth h (i.e., at the bottom of the base layer) (N/m^2).

In Eq. 20, it is assumed that the axle is long enough that the pyramids related to the two dual wheels do not interfere. This assumption is valid for most values of α and h typically considered.

The determination of the load distribution angle of a geogrid-reinforced base layer is discussed later.

Influence of the Tensioned Membrane Effect

As explained previously the normal stress is not the same on both sides of a reinforcing element exhibiting a tensioned

membrane effect. Consequently, the vertical stress on the lower (convex) side of the geogrid under the wheels is:

$$p = p' - p_m \qquad (21)$$

where: p' = vertical stress on the upper (concave) side of the geogrid given by Eq. 20 (N/m^2); and p_m = normal stress difference between the two sides of the geogrid resulting from the tensioned membrane effect (N/m^2).

The magnitude of the tensioned membrane normal stress, p_m, has been evaluated by Giroud and Noiray (1981) as a function of the tensile stiffness and elongation of the reinforcement and the shape of the deformed surface of the subgrade soil.

Combined Influence of the Three Effects

The equations presented above for the three effects, confinement, load distribution and tensioned membrane effect, are combined to obtain the ratio $R = h/h_o$ ("thickness ratio") between the thicknesses of the base layer with and without reinforcement respectively.

Eliminating γ between Eqs. 14 and 15 written for a load P (i.e., replacing P_s and h_{os} by P and h_o, respectively), and Eqs. 19 and 20, p' between Eqs. 20 and 21, and c_{uN} between Eqs. 15 and 19, and solving the resulting quadratic equation lead to:

$$R = h/h_o = \left[\sqrt{(B-L)^2+4Y} - (B+L)\right]/(4h_o \tan\alpha) \qquad (22)$$

where: R = thickness ratio (dimensionless); h and h_o = thicknesses (m) of the base layer with and without reinforcement, respectively, for an axle load P; B and L = width and length respectively of the rectangular area replacing the actual contact area between a dual wheel and the surface of the base layer (m); α = load distribution angle of the reinforced base layer; and Y = term given by Eq. 23 (m^2):

$$Y = 1/\left[(1+2/\pi)/(B+2h_o\tan\alpha_o)(L+2h_o\tan\alpha_o)+2p_m/P\right] \qquad (23)$$

where: P = axle load (N); B and L = width and length, respectively, of the rectangular area replacing the actual contact area between a dual wheel and the surface of the base layer (m); and h_o and α_o = thickness and load distribution angle, respectively, of the unreinforced base layer; and p_m = normal stress difference between the two sides of the geogrid (N/m^2).

As noted previously, the value of p_m is obtained from several lengthy equations, making it impractical to prepare a limited number of simple charts if p_m is taken into account. However, Y (and consequently R) are simplified if p_m is neglected. Systematic comparisons of values of R calculated with and without p_m have shown that: (i) if the rut depth is 0.075m the effect of p_m on R (hence on the design thickness of the base layer) is negligible; and (ii) if the rut depth is 0.15m, the value of R calculated with p_m is approximately 10% smaller than the value of R calculated neglecting p_m, regardless of the other parameters.

Consequently, in the design method presented hereafter, the normal stress difference, p_m, resulting from the tensioned membrane effect is neglected, and when it is not negligible a lump reduction of 10% of the design thickness of the base layer is recommended.

Values of the thickness ratio, R, calculated using Eqs. 22 and 23 with $\tan\alpha_o = 0.6$ are presented in Fig. 8. These values were obtained using values of B and L corresponding to a tire inflation pressure of 620 kN/m^2. However, almost identical values are obtained for a wide range of tire inflation pressures, provided the thickness of the base layer is at least 0.15m.

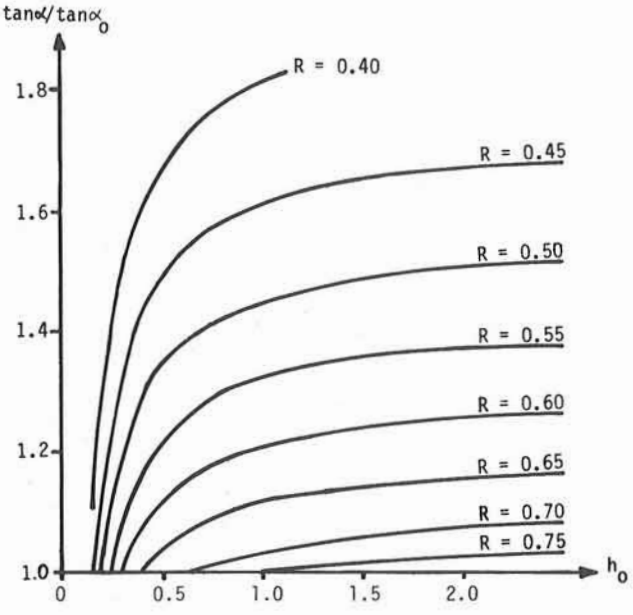

Fig. 8 Thickness ratio, R, versus load distribution improvement ratio, $\tan\alpha/\tan\alpha_o$, and thickness of unreinforced base layer, h_o.

For simplicity, a single value of $\tan\alpha_o$ (0.6) was used for calculation of R. A parametric study using a range of values for $\tan\alpha_o$ (0.4 to 0.8) showed that R was only slightly influenced by $\tan\alpha_o$, particularly for h_o values greater than 0.3m. Thus, while it is recognized that a value of $\tan\alpha_o$ of 0.6 may not represent the actual stress distribution, it has little influence on the ratio $\tan\alpha/\tan\alpha_o$ and therefore little influence on the calculated thickness of aggregate.

To use Fig. 8 to determine the thickness ratio, R, for design of a reinforced unpaved structure, the load distribution angle, α, corresponding to the considered reinforcement must be established. The purpose of the next section is to present an approach for determining α.

STUDY OF THE LOAD DISTRIBUTION ANGLE

Purpose and Approach

The purpose of reinforcing a base layer is to increase its load distribution capability by improving its mechanical properties. Improving the mechanical properties of the base layer does not necessarily mean improving the properties of the base layer as constructed. It means ensuring that the properties of the base layer after a given number of passages are superior to the properties that the base layer would have had without reinforcement after the same number of passages. This can be achieved if the reinforcement prevents or delays deterioration of the base layer in addition to, or instead of, improving the properties of the base layer as constructed.

The analyses presented below have been conducted to evaluate the effectiveness of geogrids in improving the mechanical properties of base layers and preventing their degradation.

Scope of Elastic Analyses

Linear elastic theory has been used to describe the behavior of all materials involved: base layer material subgrade soil and geogrid. Although in reality the subgrade is loaded at the plastic limit, elastic analyses were conducted because elastic theory allows the vertical stresses to be calculated with reasonable accuracy and because it is the simplest way to evaluate the effect of a variety of parameters such as:

- Material properties: elastic moduli of base layer material and subgrade soil; tensile stiffness of the reinforcement; effect of contamination and/or very low confining stress on base layer material .
- Geometry: thickness of base layer, thickness of deteriorated base layer, location of reinforcement.

To simplify the analyses, a dual-wheel load of 40 kN was represented by a pressure uniformly distributed over a circular area, 0.3m in diameter. This load was applied at the surface of a multilayer soil system representing a base layer on a subgrade (Fig. 9). Several cases were considered in order to evaluate the effect of reinforcement on the load distribution angle. For all cases the subgrade soil was the same: a saturated clay with a Young's modulus of 10 MN/m^2 and a Poisson's ratio of 0.5.

Two cases of unreinforced base layer were considered (A and B in Fig. 9). In both cases, the bottom part of the base layer consisted of a contaminated aggregate under zero confining stress. The top part of the base layer consisted of clean aggregate in case A and contaminated aggregate in case B.

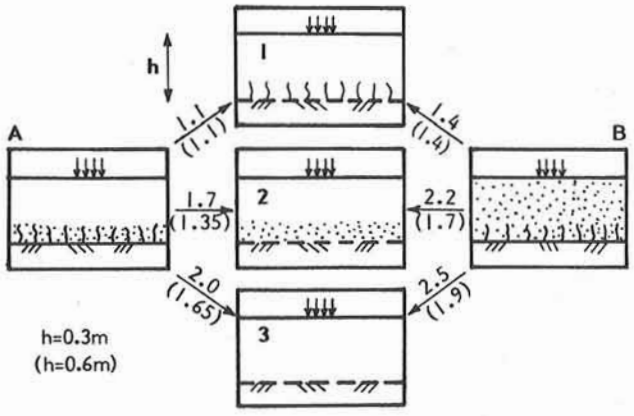

Fig. 9 Summary of elastic analyses showing the considered cases (A and B = unreinforced; 1, 2 and 3 = reinforced), values of the moduli (E_h, horizontal, and E_v, vertical), and values of the load distribution improvement ratio $\tan\alpha/\tan\alpha_o$ (written above the arrow for h = 0.3m and under the arrow, in parenthesis, for h = 0.6m) (h is the thickness of the base layer; σ_c = 0 means zero confining stress.)

Three cases of reinforced base layer were considered (1,2, and 3 in Fig. 9):

- In case 1, the reinforcing element provides separation, thus preventing contamination, but negligible reinforcement, thereby permitting a large reduction in confining stress as the base layer deforms vertically and laterally.
- In case 2, the reinforcing element provides reinforcement of the base layer. Aggregate/geogrid interlocking causes the confining stress on the aggregate to increase, relative to the unreinforced case, as the reinforcing element is put into tension. This prevents lateral displacement of the base layer material. In case 2, the reinforcing element is not assumed to provide separation. However, since a high confining stress in the base layer is developed, aggregate sinking and lateral displacement are limited, thereby reducing contamination.
- In case 3, the reinforcing element provides reinforcement and separation.

Values of Young's moduli used in the elastic analyses are given in Fig. 9. These values were selected as follows: 30 MN/m^2 for a clean base layer aggregate; 10 MN/m^2 for the undrained Young's modulus of a saturated clay and for the aggregate contaminated by the clay; zero for the horizontal Young's modulus of the aggregate subjected to a zero confining stress. The zero Young's modulus represents complete dissociation of the base layer aggregate due to lateral displacement.

Two base layer thicknesses have been considered in the elastic analyses: 0.3m and 0.6m. Several values for the depth of the base layer affected by contamination and zero confining stresses have been considered. In addition, a number of intermediate cases, falling within the range of conditions presented in Fig. 9, have been considered, (i.e., cases where the depth of partial contamination was different from the depth of the zone where confining stress is zero). These additional cases will not be presented in detail.

Method of Interpretation of the Elastic Analyses

The results of the elastic analyses have been interpreted as follows:

- For each case (reinforced or unreinforced), a finite element computer program is used to obtain the distribution of vertical stresses on the subgrade soil.
- For a given unreinforced case (i.e., A or B in Fig. 9), the fraction of the load encompassed by a load distribution pyramid with an angle of $\alpha_o = \tan^{-1} 0.6$ is calculated by integrating the vertical stresses at the base layer/subgrade interface, over the width of the load distribution pyramid.
- For each corresponding reinforced case (i.e., 1, 2, or 3 in Fig. 9, with the same thickness of base layer and depth of zone where confining stress is zero, if any, as in the given unreinforced case), the angle of the load distribution pyramid, α, encompassing the same fraction of the load at the base layer/subgrade interface as for the unreinforced case, is determined. The improvement of load distribution in the reinforced case compared to the unreinforced case is characterized by the ratio $\tan\alpha/\tan\alpha_o$, called load distribution improvement ratio.

A parametric study has shown that the use of 0.6 for $\tan\alpha_o$ has only a minor effect on the calculated results.

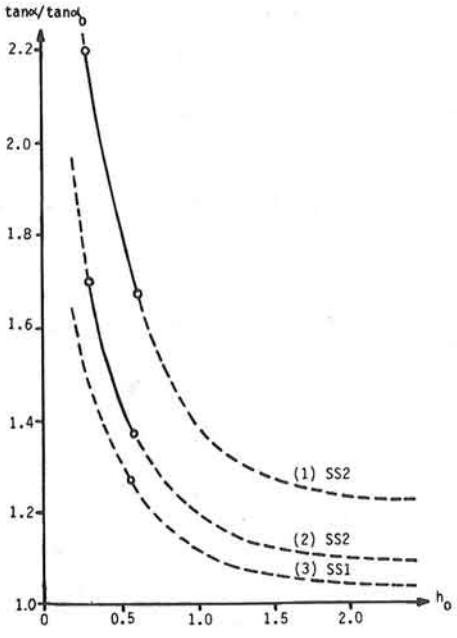

Fig. 10 Curves giving the load distribution improvement ratio, $\tan\alpha/\tan\alpha_0$, as a function of the thickness of the unreinforced base layer, h_0. Curve (1) is related to the case of a large number of passages (e.g. N larger than 1000) where significant contamination would be expected without reinforcement; and curves (2) and (3) are related to the case of a small number of passages where no significant contamination would be expected without reinforcement. Circles represent the calculated points. Dashed curves have been extrapolated.

Results of the Elastic Analyses

Results obtained for Tensar SS2 geogrid (quick loading tensile stiffness K=500 kN/m) are summarized in Fig. 9 where values of $\tan\alpha/\tan\alpha_0$ obtained as described above, with $\tan\alpha_0 = 0.6$, are indicated. The following conclusions can be drawn:

- If the reinforcing element provides separation, but only negligible reinforcement, the load distribution improvement ratio ($\tan\alpha/\tan\alpha_0$) is 1.1. to 1.4 depending on the expected degree of contamination of the base layer without reinforcement. These values of the ratio appear practically independent of the thickness of the base layer.

- If the reinforcing element provides significant reinforcement, preventing a very low or zero confining stress (and consequently limiting the extent of contamination as explained above), the load distribution improvement ratio is 1.7 to 2.2 , depending on the expected degree of contamination of the base layer without reinforcement. This range of values of the load distribution improvement ratio is for a base layer thickness of 0.3m. For a thickness of 0.6m, the range of values is 1.35 to 1.7. These results indicate that the effectiveness of a given reinforcing element (i.e., a reinforcing element with a given tensile stiffness) decreases as the thickness of the base layer increases.

- If the reinforcing element provides separation and reinforcement, the load distribution improvement ratio becomes large (2.0 to 2.5 for a thickness of 0.3m and 1.65 to 1.9 for a thickness of 0.6m, as shown in Fig. 9).

In addition, calculations made with a base layer thickness of 0.6m result in a multiplier of 1.25 for Tensar SS1 geogrid (tensile stiffness K = 300 kN/m) instead of 1.35 for Tensar SS2 geogrid (tensile stiffness K = 500 kN/m) for the case A2 (reinforcement without separation).

From these results, three curves can be tentatively drawn as shown in Fig. 1: curve (1) related to Tensar SS2 geogrid for the case of a large number of passages (e.g., N larger than 1000) for which significant contamination would be expected without reinforcement; curve (2) related to Tensar SS2 geogrid and curve (3) related to Tensar SS1 geogrid for the case of a small number of passages for which no significant contamination would be expected without reinforcement.

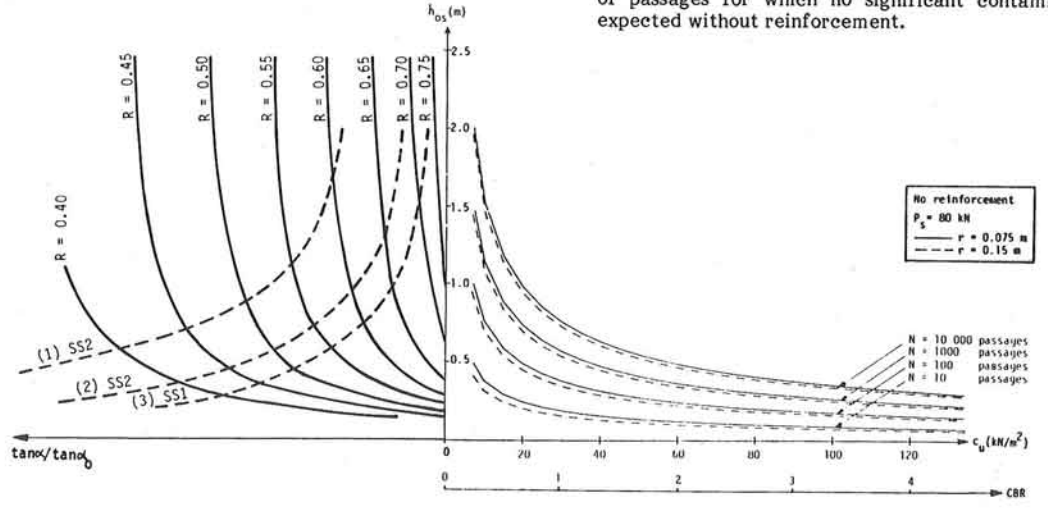

Fig. 11 Chart for the design of geogrid-reinforced unpaved structures. (Fig.11 combines Fig.4,8 and 10.)

DESIGN METHOD AND EXAMPLE

Proposed Tentative Design Method

Geogrid reinforced unpaved roads or areas can be designed using the chart presented in Fig. 11, valid for a standard axle load (P_s = 80 kN). Similar charts have been developed for other axle loads. Four steps are necessary:

- o First step - Given the subgrade undrained shear strength, c_u, the number of passages, N, and the allowable rut depth, r, (0.075 m or 0.15 m), determine the thickness, h_o, of the unreinforced base layer using the right part of Fig. 11.
- o Second step - Select in the left part of Fig. 11 the dashed curve related to the considered type of geogrid: Tensar SS1 or Tensar SS2.
- o Third step - At the intersection of the selected dashed curve and the thickness h_o, interpolate for the thickness ratio, R, between two solid curves.
- o Fourth step - Determine the thickness of the Tensar reinforced aggregate layer as follows:

$$h = R\, h_o \quad (23)$$

(if rut depth is less than 0.15m and/or traffic is not channelized).

$$h = 0.9\, R\, h_o \quad (24)$$

(if rut depth is 0.15m or more and if traffic is channelized; i.e., 0.9 accounts for tensioned membrane effect)

Design Example

The use of the proposed tentative design method is illustrated by the following design example.

An unpaved road consisting of an aggregate base layer is to be built on a subgrade soil with a CBR value of 0.3 . The expected traffic during the design life of the unpaved road is 1000 passages of trucks whose front axle load is negligible and rear axle load is the American-British standard axle load. The allowable rut depth is 0.075m.

The undrained cohesion of the subgrade soil can be derived from the CBR using Eq. 8:

$$c_u = 0.3 \times 30\,000 = 9\,000\ N/m^2 = 9\ kN/m^2$$

Using the right part of Fig. 11 for a rut depth r = 0.075m and a number of passages N = 1000, gives the design thickness of a unreinforced unpaved road for the American-British standard axle load (P_s = 80 kN): h_{os} = 1.20m.

Using the left part of Fig. 11 for h_{os} = 1.20m, and the curve (1) related to Tensar SS2 geogrid for a large number of passages, gives the following value of the thickness ratio: R = 0.55.

Since the allowable rut depth is less than 0.15m, Eq. 23 should be used to determine the thickness of the geogrid-reinforced unpaved road:

$$h = 0.55 \times 1.20 = 0.66m$$

If the geogrid had not improved the load distribution capability of the base layer, and had only provided confinement, the value of the thickness ratio would have been read on the axis of Fig. 11 for $\tan\alpha/\tan\alpha_o = 1$: R = 0.76. Hence:

$$h = 0.76 \times 1.20 = 0.91m$$

CONCLUSIONS

Understanding of the Behavior of Unpaved Structures

The behavior of unpaved structures is complex because of the variety of phenomena involved. Little help can be provided by existing technical literature due to a lack of well documented observations on the behavior of unpaved structures. Observations of unpaved structure behavior are difficult because of the large number of parameters and, because unpaved structures, which are often temporary, are seldom instrumented and/or monitored, in contrast to permanent structures such as high vertical retaining walls.

Because of the lack of data from observations, conceptual models constitute a useful attempt at understanding the behavior of unpaved structures. From that viewpoint, this paper provides a detailed discussion on the behavior of unreinforced and reinforced unpaved structures, intended to identify and describe the mechanisms involved and their relationships. The paper also presents analyses to tentatively quantify the influence of some of the identified mechanisms. For instance : (i) elastic analyses were used to provide an evaluation of the influence of contamination and low confining stresses on the load distribution capability of a base layer; (ii) calculations have been carried out to compare the influence of subgrade soil deterioration and base layer deterioration on full-scale test unpaved road behavior; and (iii) the relative importance of the various mechanisms by which reinforcement improves the behavior of an unpaved structure, such as confinement of the subgrade soil, load distribution and tensioned membrane effect have been evaluated.

Relevance to Geogrids of the Proposed Tentative Method

The design method presented in this paper includes several mechanisms by which geogrids can improve unpaved structure behavior, in particular the improvement in load distribution capability of the base layer that geogrids are expected to provide. Calculations presented in this paper show that :

- o Improvement of load distribution capability of the base layer is one of the two mechanisms that provide most improvement to unpaved structures, among the identified mechanisms (it is therefore important to use reinforcing elements improving the base layer load distribution capability), the other mechanism being subgrade soil confinement.
- o Through interlocking with base layer material (especially if this material is aggregate) geogrids can provide significant improvement in base layer load distribution capability. Such improvement does not significantly result from the increased stiffness provided by the geogrid to the base layer as constructed, but results mostly from the fact that a geogrid, through interlocking with base layer material (especially if this material is aggregate) reduces or delays the mechanisms of deterioration of unpaved structures (i.e. decrease of effective thickness and decrease of properties of base layer, associated with increasing number of vehicle passages).

A conclusion that can be tentatively drawn from the proposed tentative design method is that the savings in base layer thickness is not proportional to the tensile stiffness of the geogrid. Such a conclusion should not be surprising since in an unpaved structure, base layer material/geogrid interaction is at least as important as geogrid tensile stiffness.

Discussion of the Results

Systematic calculations similar to the above presented design example show that the thickness of unreinforced unpaved

structures can be reduced by 30 to 50% by using existing geogrids.

As is usual for the design of unpaved structures, base layer thickness values do not include a factor of safety. In addition, these values should be considered with caution because the method has not yet been calibrated with either small-scale or full-scale test data.

The calculations also show that approximately half of the thickness reduction resulting from geogrid reinforcement is due to subgrade confinement and approximately half of the improvement is from improved load distribution resulting from geogrid-base layer material interlocking.

Suggested Developments

The following developments and additional research work are suggested:

- Systematic elastic analyses, using the approach described in this paper, encompassing a wide range of parameters having an influence on the base layer load distribution capability (especially the base layer thickness). (The elastic analyses presented in this paper should be considered as an attempt at defining an approach and obtaining preliminary results.)
- Elastic analyses similar to the above with several layers of geogrids in the base layer.
- Calibration of elastic analyses with data from small-scale model tests.
- Review of laboratory test data on fatigue of clay caused by repeated loadings to refine the evaluation of the relative importance of base failure versus subgrade failure.
- Detailed study of full scale tests that have been conducted on unpaved structures to evaluate the relative importance of the various mechanisms of failure.
- Evaluation of field installations and field tests on unreinforced and geogrid-reinforced unpaved roads.
- Adaptation of the proposed tentative method to a variety of subgrade soils, such as peat, loose sand and frozen soils, and a variety of base layer materials.

ACKNOWLEDGEMENTS

The research into unpaved road behavior and the development of a design method for geogrid-reinforced structures was started when all of the authors were members of the Geotextiles and Geomembranes Group of Woodward-Clyde Consultants. The authors are indebted to J. Dixon for valuable comments, and S. Hartmaier and N. Stuart for assistance in the preparation of this paper. The authors thank Gulf Canada Ltd. for their support throughout the course of this study and Netlon Ltd. for the opportunity to participate in the Soil Reinforcement Design Group which, under the chairmanship of Sir Hugh Ford, provided a catalyst for the development of design procedures for geogrid-reinforced structures.

REFERENCES

Giroud, J.P., "Discussion and closure on Geotextile - Reinforced Unpaved Road Design", Journal of the Geotechnical Division, ASCE, Vol. 108, No. GT 12, (December 1982), 1654-1670.

Giroud, J. P., and Noiray, L., "Geotextile-Reinforced Unpaved Road Design", Journal of the Geotechnical Division, ASCE, Vol. 107, No GT9, Proc. paper 16489, (September 1981), 1233-1254.

Hammit, G., "Thickness Requirements for Unsurfaced Roads and Airfield Bare Base Support," Technical Report S-70-5, United States Army Engineer Waterways Experiment Station, Vicksburg, Miss., (July, 1970).

McGown, A., and Andrawes, K.Z., "The Influences of Nonwoven Fabric Inclusions on the Stress Strain Behaviour of a Soil Mass", Proceedings of the International Conference on the Use of Fabrics in Geotechnics, (Paris, 1977), 161-166.

Raymond, G. P., and Hayden, F.B., "Effect of Reinforcement on Sand Overlying Bases of Different Compressibilities Subject to Repeated Loading," C.E. Research Report No. 79, Department of Civil Engineering, Queens University, Kingston, Ontario, (Nov., 1983).

Webster, S. L., and Alford, S. J., "Investigation of Construction Concepts for Pavements Across Soft Ground," Technical Report S-78-6, United States Army Engineer Waterways Experiment Station, Vicksburg, Miss., (July, 1978).

Webster, S. L., and Watkins, J. E., "Investigation of Construction Techniques for Tactical Bridge Approach Roads Across Soft Ground," Technical Report S-77-1, United States Army Engineer Waterways Experiment Station, Vicksburg, Miss., (Feb., 1977).

NOTATION

Symbols used in the design method are as follows:

- CBR = California Bearing Ratio of the subgrade soil (dimensionless);
- c_u = undrained shear strength (cohesion) of the subgrade soil (N/m^2);
- h = reinforced base layer thickness (m) corresponding to an axle load P;
- h_o = unreinforced base layer thickness (m) corresponding to an axle load P;
- h_{os} = unreinforced base layer thickness (m) corresponding to a standard axle load P_s;
- N = number of passages of axle during design life of the structure (dimensionless);
- P = axle load (N);
- P_s = American-British standard axle load (80 kN);
- R = h/h_o = thickness ratio (dimensionless);
- r = rut depth (m);
- α = load distribution angle for reinforced base layer;
- α_o = load distribution angle for unreinforced base layer; and
- $\tan\alpha/\tan\alpha_o$ = load distribution improvement ratio.

Model testing of geogrids under an aggregate layer on soft ground

The mechanisms by which the inclusion of a geogrid may improve the performance of unpaved roads and similar constructions are being studied at reduced scale by laboratory model tests. Tests so far have been conducted under plane strain conditions by applying monotonic loading from a rigid footing to reinforced and unreinforced soil-aggregate systems, using a range of fill thicknesses and subgrade strengths. Performance of the reinforced systems is significantly better, primarily because the grid effectively resists the tensile strains which develop in the base of the aggregate layer.

G. W. E. Milligan and J. P. Love, *Oxford University*

INTRODUCTION

It is a common construction technique to place a layer of coarse granular material on the surface of weak and compressible ground, for the formation of unpaved roads, working areas, parking lots, storage areas and the like. The design problems for such constructions vary with their purpose; they may be concerned with foundation failure under local concentrated loading, or with trafficking problems due to rutting. What they generally have in common is that they involve structures with a relatively limited life, in which larger-than-usual deformations are expected and acceptable, and on which the loading is often localised, variable, repeated, or moving, or some combination of all of these.

Such construction is difficult to design precisely, yet the use of very conservative methods may have severe financial implications; on the other hand, failures may also prove very expensive in terms of loss of access, machine down-time or time spent on repair work. One method of improving the construction which has found rapidly-increasing use is to incorporate either a geotextile or a geogrid at the base of the aggregate by laying it on the surface of the ground before placing the aggregate. Not only may this allow a reduced thickness of fill to be used but should improve the reliability of performance by increasing substantially the load required to cause a complete failure of the soil-aggregate system. The performance limit for the system is then even more likely to be one of excessive deformation or rutting than of ultimate failure; the life of the structure may then be readily extendible as required by simple maintenance such as filling of ruts or regrading.

There is now much field evidence of the benefits of using a geotextile in such a system, but there is still no generally accepted design method. It is recognised that the fabric has three main functions:

(i) Separation of the aggregate fill from the soft ground.

(ii) Membrane action.

(iii) Reinforcement.

It seemed possible that the latter two functions at least might be performed better by a Tensar geogrid than a geotextile as it is generally stiffer and forms a positive interlock with the aggregate (Jewell et al 1984). The primary aim of the work reported in this paper was to investigate the performance of a Tensar geogrid in such a situation. By observing carefully the mechanisms of deformation and failure it was also intended that the relative merits of proposed general methods of design of soil-aggregate systems could be assessed and some progress made towards a generally acceptable method.

MODEL TESTING

As already noted above this is a difficult problem, because loading conditions are complex and pre-failure deformations, and hence the stiffness as well as strength of all the materials involved, are highly important. Even if attention is restricted to the access road, in which vehicles generally follow a single path and the problem is reduced to the rate at which ruts develop, there are many variables to consider: vehicle weight, axle configuration and tyre pressure; fill type and thickness; reinforcement type, strength and stiffness; and the geotechnical properties of the subgrade. Under site conditions the effects of construction technique such as the method of laying the reinforcement and compacting the fill, may also be highly significant. As a result much of the information obtained to date has been specific to a particular site and method of construction.

Polymer grid reinforcement. Thomas Telford Limited, London, 1985

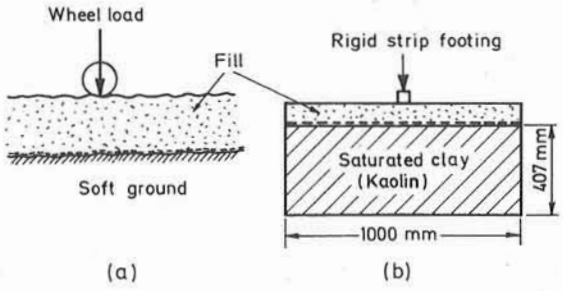

Fig 1.
Field problem Idealised model

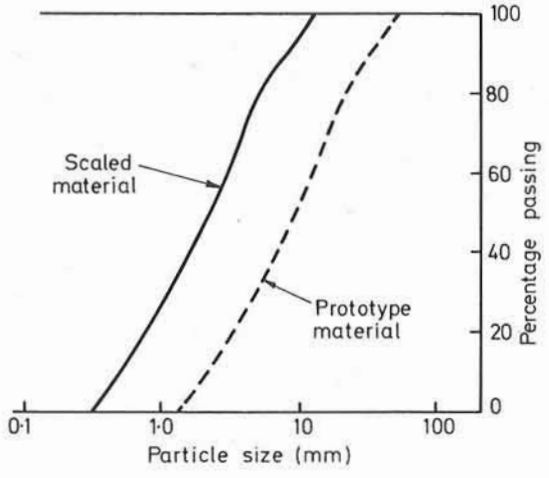

Fig 2. Grading of fill material

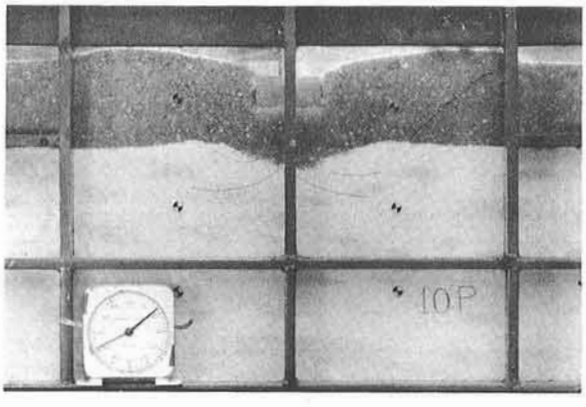

Plate 1. View through side of apparatus (end of test)

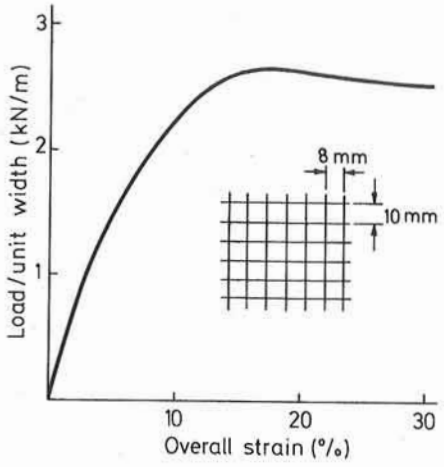

Fig 3. Properties of grid material

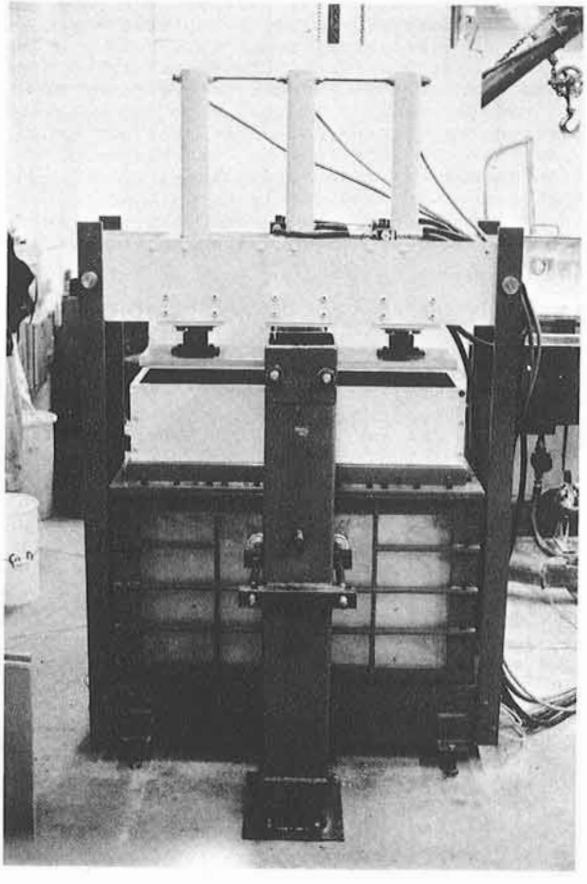

Plate 2. Apparatus during consolidation stage

A decision was therefore made to work in the laboratory, performing model tests at approximately one quarter scale, to allow variables to be controlled more precisely and more accurate measurements to be made. The problem was also simplified initially as far as possible by investigating the behaviour under plane strain conditions of soil-aggregate and soil-fabric-aggregate systems loaded monotonically by a rigid footing (see Figure 1). A single type of subgrade soil (saturated kaolin clay), a single type of reinforcement (Tensar SS-type geogrid), and a single type of fill (type 2 sub-base material as specified by the Department of Transport), have been used. The principal variables investigated to date have been the depth of the aggregate layer and the strength of the subgrade soil.

Working at small scale introduces problems in the correct physical modelling of all aspects of the problem. Modelling need not in all cases be perfect; a common use of small scale physical modelling is to investigate general mechanisms of behaviour and hence suggest an appropriate analytical model which can then be applied to the full-scale problem, and this has been one purpose of the tests reported here. However, the analytical model must take proper account of all important parameters if it is to respond correctly to changes in behaviour from small to full scale. In this case the relative importance of various parameters was not known in advance; in addition, in the absence of a design method, it might prove possible to extrapolate results directly to full scale. An attempt has therefore been made to model the various components of the system as accurately as possible.

Dimensional analysis indicated that for correct modelling all dimensions, loadings, material strengths and material stiffnesses should be reduced by the geometrical scale factor of four. To meet the first condition the depth of fill was reduced, the range of 50 to 100mm corresponding to a realistic range of 200 to 400mm in the field, and the particle sizes in the aggregate scaled down as shown in Fig. 2. A miniature Tensar geogrid was produced by Netlon Limited to model the grid; the scale dimensions were in practice between those of SS1 and SS2 grids, and some difficulty was experienced in obtaining a regular grid with repeatable properties. Average dimensions and properties of the grid used are shown in Fig. 3. Particle size in the clay subgrade was considered to be of no significance since it was much smaller than the fill particle size and the grid aperture size at both full and model scale.

The stiffness and strength of the subgrade was taken to be characterized by a single parameter, the undrained shear strength. This is certainly appropriate for the strength, since the loading considered was rapid and any failure would take place under undrained conditions. For normally-consolidated clays the undrained stiffness is approximately proportional to the undrained shear strength. In these tests the method of preparation of the clay was such that it was overconsolidated to a greater or lesser extent and it is probable that the stiffness varied less than in proportion to the shear strength, being relatively higher for the softer than for the stiffer clays. Subgrades with nominal strengths of 6, 10 and 16 kN/m^2 were used, corresponding to field strengths of 24, 40 and 64 kN/m^2. Ideally an even lower strength of say 10 - 12 kN/m^2 at full scale should also have been used, but the resulting scaled subgrades were impossibly soft to work with.

The material properties of the Tensar grid were a major difficulty. The method of manufacture was such that the properties of the aligned polymer could only be modified to a relatively small degree by the use of different polymers and variations in the draw ratio. Several types of grid, both oriented and non-oriented, were investigated. Finally use was made of the variation of Tensar properties with strain-rate to produce the scaling effect. The miniature grid was tested at a wide range of different strain-rates; both initial stiffness and peak strength decrease with reducing strain rate. An estimate was made of the typical strain-rate in a layer of fabric under a moving wheel load, and a rate of loading in the tests adopted which would give approximately the right reduction in fabric stiffness.

Modelling of the properties of the fill also caused some difficulty. In a frictional material the strength is automatically reduced in proportion to the ambient stresses, except that at low stress levels the angle of internal friction generally increases. This can be counteracted by using a slightly less dense material, which also helps to make the modelling of the shear modulus more accurate since this has been found to reduce less rapidly than in direct proportion to the stress level (Wroth et al. 1979). In practice however, it was found to be difficult to compact the fill on top of the soft clay and the degree of compaction achieved was probably somewhat less than would have been theoretically ideal.

APPARATUS AND METHOD OF TESTING

The main part of the apparatus is a strong box with internal dimensions of 1000 mm in length, 300 mm width and 600 mm depth. The ends and base are of aluminium plate and the sides, of 25 mm thick perspex, are supported by steel frames. The clay subgrade is formed as a block of kaolin approximately 400 mm deep by consolidation from a slurry. The initial volume of kaolin is about double the final volume so an extension box fits on top of the test box for the consolidation stage. The complete box fits inside a loading frame and the clay is consolidated by a rigid platen driven by three hydraulic cylinders operated by compressed nitrogen. Additional supports to the sides of the tank are provided during the consolidation stage to help resist the high lateral pressures. Drainage is allowed from the top and bottom but not the sides of the sample.

Once the kaolin has been consolidated to the required extent the platen is removed and the clay allowed to swell back under water until an

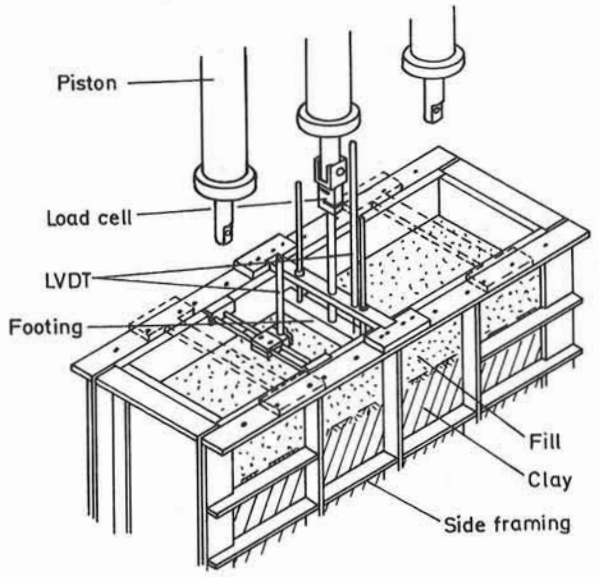

Fig 5. Apparatus for tests

equilibrium state is achieved. One side of the tank may also briefly be removed to allow a grid of markers to be placed on the side surface of the clay. These are visible through the perspex side wall and allow deformations in the clay to be observed during a test. The resulting sample of clay is not uniform and one full sample of each of the nominal strengths of clay used has been set aside for a thorough investigation of the variation of moisture content and undrained strength throughout the block. Typical results for one such investigation are given in Fig. 4 and Table 1.

Immediately before the test the surface of the clay is scraped to produce a flat, level surface. If a Tensar grid is to be incorporated it is then laid on the surface of the clay, without pretensioning. Fill is then placed in layers to the required depth with careful compaction by hand tamping. The fill is placed at about optimum moisture content; capillary suctions in a damp unsaturated fill will obviously be more significant at the model scale than at full scale, but dry fill was found to draw up moisture from the clay to a variable degree while attempts to work with the fill inundated were not successful.

Spot levels on the surface of the fill are taken at a grid of points in plan to obtain an accurate measurement of the thickness of the fill at the start of the test. This procedure is repeated at the end of the test to check the surface heave.

The tests themselves consist of driving a rigid footing into the fill at a constant rate using one of the hydraulic rams, as shown in Fig. 5. Footings of various widths have been used but for the main series of tests the width was 75mm, equivalent to 300mm at full scale. The rate of descent is controlled by having the low-pressure

	Undrained Shear Strength, Cu (kN/m^2)			Moisture Content (%)	
Depth, mm	SV1	SV2	SV3	MC1	MC2
70	7.4(10)*	6.8(7)*	6.6(7)*	60.1	60.3
170	9.0	8.2	7.2	59.0	59.6
270	9.4	9.2	9.3	58.0	58.3
370	9.4	10.0	10.1	57.6	58.3

* corresponding values of Cu from triaxial tests

Table 1. "Site investigation" results

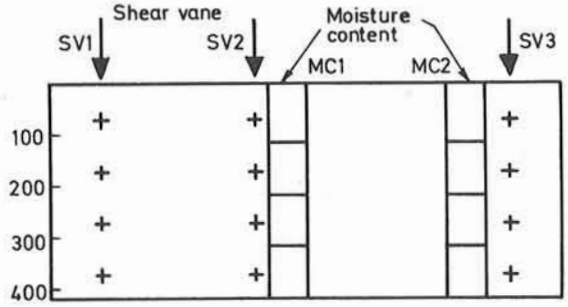

a) Location of tests

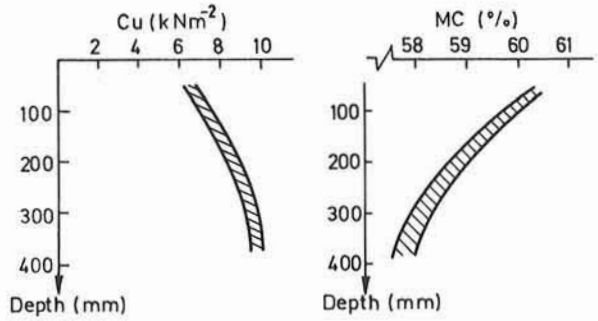

b) Profiles of shear strength and moisture content

Fig 4. Typical "site investigation" (for Cu 6 kN/m^2)

H(mm)	50	75	100	Reinforcement (a) without grid (b) with grid
Cu(KN/m^2)				
6	17P	8P	10P	(a)
	17TM	8TM	10TM	(b)
10	9TM	7P,14TM	12TM,15TM	(a)
	9P	14P	12P,15P	(b)
16	13TM	16P	11P	(a)
	13P	16TM	11TM	(b)

Table 2. Test numbers

side of the cylinders filled with hydraulic fluid which is allowed to flow out through a constant-flow-rate device, the high pressure side again being supplied from compressed nitrogen cylinders. The load on the footing is measured by an electrical load cell and its displacement by an LVDT. The test is stopped automatically when the footing has descended 50mm, equivalent to 200mm at full scale.

The primary test position is obviously in the centre of the box using the middle hydraulic cylinder, but secondary tests may subsequently be performed at either end using the outer cylinders. These are generally found to give somewhat higher loads due to the proximity of the rigid end walls of the box. Secondary tests were used initially to investigate the effects of different sizes of footing and to check on the repeatability of results. Latterly it has become the standard test procedure to use the secondary test positions to check the strength of the clay sample, by performing a load test with the footing directly on the clay (after removal of the fill) at one end and performing laboratory vane tests and taking samples of clay for triaxial testing and moisture content determination from the other.

The depth of clay affected by the tests is relatively small and it has proved possible to perform a series of tertiary tests using the bottom 200mm depth of the clay after removing the top 200mm and again allowing swelling under water to occur before placing the geogrid, if used, and the layer of aggregate. In fact the middle tertiary tests have given results which agree closely with the primary ones in directly comparable tests; the results of tertiary middle tests are therefore considered to be as reliable as those from the primary tests.

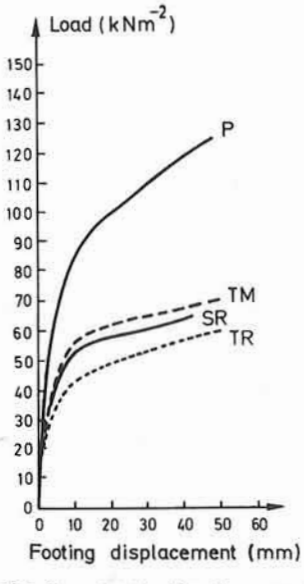

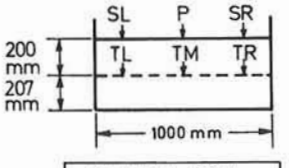

SAMPLE Nº 14			
Subgrade Cu=10 kN/m^2			
Test	Footing width (mm)	Fill depth (mm)	Grid
P	75	75	✓
SR (SL	75 No test	—	—)
TM	75	75	—
TR (TL	75 No test	—	—)

Fig 6. Load-displacement curves from one sample

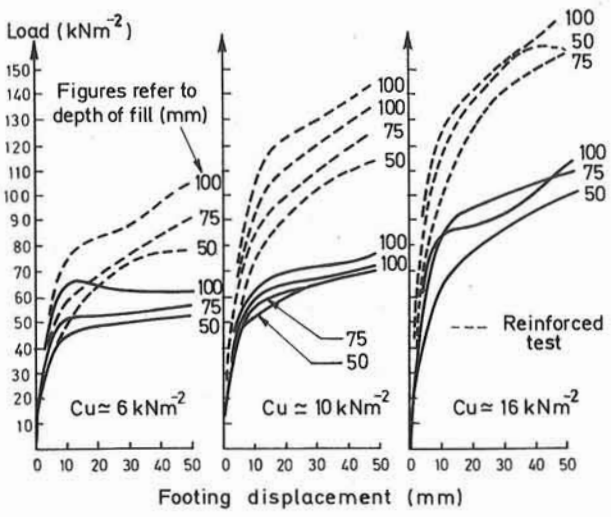

Fig 7. Load-displacement curves: summary plot

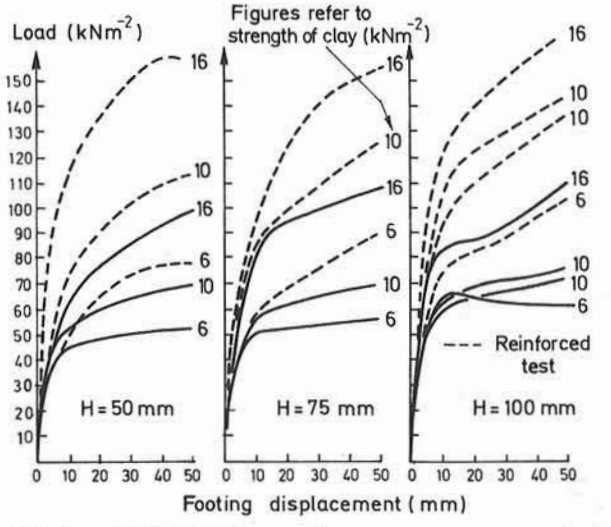

Fig 8. Load-displacement curves: summary plot

In addition to measurements of the load on and displacement of the footing, continuous recordings are made of the heave of the fill to either side of the footing using LVDT's. At intervals during the test, which lasts for only about 30 seconds (ensuring that the response of the clay subgrade is substantially undrained) photographs are taken through the side of the box. These are subsequently used to measure the movements of the surface of the fill, the surface of the clay subgrade and the markers embedded in the clay and attached to the grid, and to observe the positions of shear planes within the clay subgrade. Reference markers for these photographs are fixed to the side wall of the tank. Readings from all transducers are recorded by a computer-controlled system and stored on disc for subsequent analysis. Some use has also been made of video film to record tests to allow subsequent review of any part of a test.

For instance, to check whether the grid is being pulled from beneath the fill rather than straining locally under the load, light rods are tied to the ends of the grid and project vertically through the fill. The stage in a test at which these start to move may be observed on a video film; displacement mechanisms in the fill are also identified more clearly by repeated viewing.

RESULTS

The results presented here are for the main series of tests, details of which are given in Table 2; the numbers indicate the successive samples of clay prepared, and the letters P and TM denote the primary and tertiary middle test positions respectively. A typical series of plots, from tests on a single sample, of the load on the footing against its vertical displacement into the fill are shown in Fig.6. The curves for loading directly onto the subgrade (SR and TR) indicate that in this case the clay was somewhat weaker for the tertiary than for the primary/secondary level. Nevertheless, it can be seen that the layer of aggregate produces a relatively small improvement in performance (TM compared with TR) while inclusion of the grid reinforcement has a very marked effect (P compared with SR). A summary of all such load/displacement curves for the tests in the central position, with and without reinforcement, is presented in Fig. 7. The same data are replotted in Fig. 8 as sets of curves for constant fill thickness rather than constant subgrade strength.

In spite of minor variations in subgrade strength within individual samples, and some differences in fill grading and density between tests, a number of clear trends appear. In all cases the failure load, defined as the load at which displacement started to increase rapidly, is approximately equal to 5 c_u for footings bearing directly on the subgrade. An unreinforced layer of fill increases the bearing capacity, quite markedly for the softest subgrade, less so for the stronger ones. Although the bearing capacity increases with fill thickness for any one subgrade strength it does so less rapidly than might be expected. The response of these unreinforced systems tend to become more 'brittle' as the subgrade strength is reduced; on the stronger subgrades the load continues to increase after initial failure, while on the weak subgrade it remains constant or even reduces. In the field a failure in such a system is likely to be fairly serious, with the load punching right through the fill into the soft clay, and difficult to repair satisfactorily.

The systems incorporating a geogrid show in all cases a marked improvement in performance. Failure loads are typically about 40% higher than for unreinforced systems; however, failure loads are much less easy to identify for reinforced systems, as the loads continue to increase quite steadily with further displacement. The performance of such a system will generally be limited by excessive deflection rather than a catastrophic failure unless the

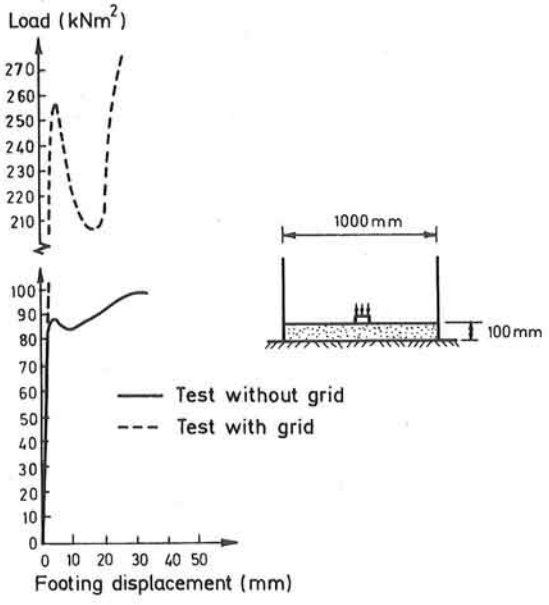

Fig 9. Load-displacement curves with no clay

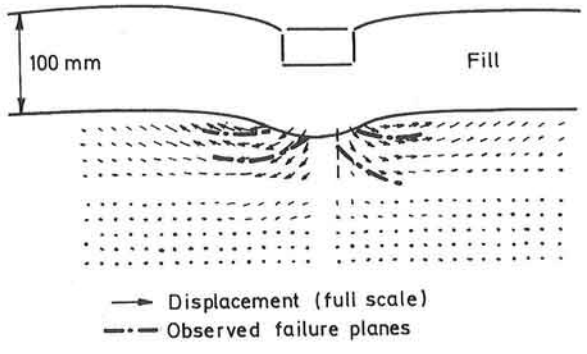

Fig 10. Displacement vectors in clay: unreinforced system

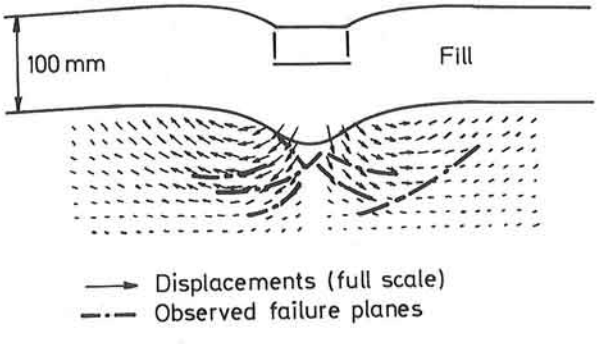

Fig 11. Displacement vectors in clay: reinforced system

reinforcement breaks. In these tests the reinforcement always remained intact. Performance clearly improves with subgrade strength, and greater benefit is obtained from using thicker fills than with unreinforced systems. The initial stiffness of the system (the slope of the load/displacement curve) increases with the strength of the subgrade and also to some extent with the thickness of the fill. For loads up to about 50% of the failure load for unreinforced systems there is very little difference in performance between the reinforced and unreinforced systems; for higher loads the stiffness of the unreinforced system reduces quite rapidly as plastic flow begins to occur in the subgrade clay.

Tests on samples 12 and 15 were nominally identical, with a subgrade strength of 10 kN/m^2 and a fill thickness of 100mm. Curves for both are plotted in Figs. 7 and 8 and give an indication of the repeatability of individual tests. Although there is some discrepancy between the curves the repeatability is quite good considering the difficulty of preparing identical samples of soil, both subgrade and fill, and the variability in the properties of the miniature grid. In the tests using the thickest fills there was some indication that failure was occurring predominantly within the fill, at least when no grid was present. Tests were therefore conducted using 100mm of aggregate placed directly on the base of the test box, with no clay; the resulting curves are shown in Fig. 9. With no reinforcement the system response was initially very stiff, but failure then occurred suddenly with a wedge of fill being pushed out either side of the loaded footing. When reinforcement was included the performance of the system improved dramatically, very high loads being reached before failure occurred. Presumably the unreinforced system failed by soil sliding outwards along the fairly smooth base of the box; the curves for the thicker fills on the strongest clay subgrade are sufficiently similar to suggest that the failure mechanism is similar, with shearing occurring in the clay at or close to the interface with the fill. When a strong grid is present such lateral movement is prevented; the upper curve in Fig. 9 is probably an upper-bound curve for reinforced fill on an infinitely stiff and strong subgrade.

Large quantities of data have been produced on the displacements and strains within the subgrade during successive stages of most tests. These are found by digitizing the positions of the markers in the clay visible in the photographs taken during the test; displacements are found from the initial and final position of each marker and strains are calculated from the distortions of quadrilateral elements with nodes at four adjacent markers. The main use of these measurements will be for comparison with the results of finite element analyses. They have also been useful, along with observations of shear planes in the clay and of the deformed shape of the surface of the subgrade and of the fill, in clarifying the different mechanisms of behaviour of the reinforced and unreinforced systems. Typical

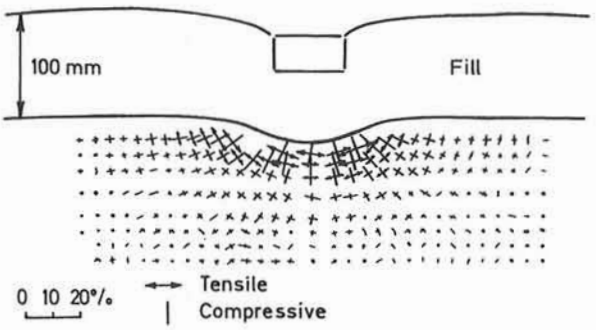

Fig 12. Strains in clay : unreinforced system

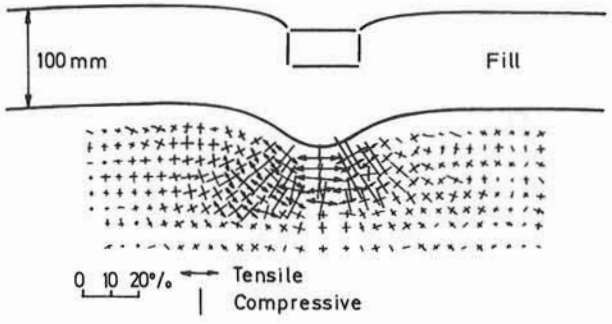

Fig 13. Strains in clay : reinforced system

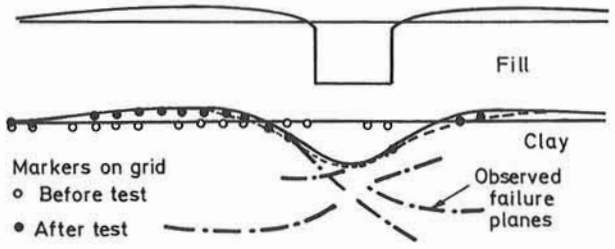

Fig 14. Displacements of markers on grid

results are shown in Figs. 10 - 13. When no grid is used the vertical displacements in the clay beheath the footing are quite small and significant displacements are restricted to a relatively limited body of clay (Fig. 10). Failure planes within the clay, made visible by the grease used to lubricate the sides of the box, are also very shallow and clearly caused by predominantly lateral movements in the clay either side of the footing. Within the fill the depth of aggregate beneath the footing is much smaller than at the start of the test. Little additional compaction has occurred and the reduction in thickness is due to lateral movement of aggregates from beneath the footing,

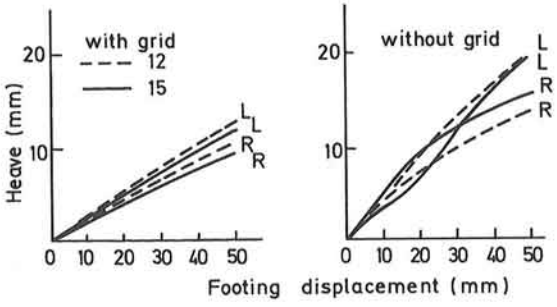

Fig 15. Measurements of surface heave

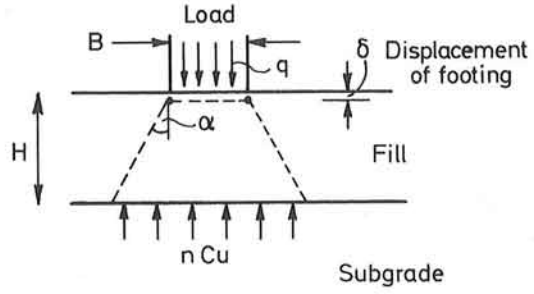

Fig 16. Simple bearing-capacity analysis

resulting in wedge-type failures in the fill either side of the footing. By the end of the test these form clearly visible outcrops in the surface of the fill. Fig. 11 shows the results for the reinforced system with the same fill depth and subgrade strength, at the same displacement of the footing (but a much higher load). Inclusion of the grid has largely prevented loss of aggregate from immediately beneath the footing and no failure planes are observed in the fill to either side. Vertical displacements in the clay beneath the footing are greater than when no grid was present, while lateral displacements in the clay are slightly reduced. Shear planes in the clay penetrate deeper into the subgrade, and the body of deforming soil is significantly greater. The deformed shape of the subgrade/aggregate interface is quite different, as is the shape of the surface of the fill.

The different deformations within the subgrade show up even more clearly in the plots of strain in Figs. 12 and 13. When no grid is used the strains are restricted to a small zone beneath the footing in which large tensile strains are developed. When the grid is used the deformed zone is much larger; large tensile strains are again observed beneath the middle of the footing, but under the edges of the footing they are very much smaller than in the unreinforced system.

These deformation measurements were obtained from tests on sample 12. Tests on sample 15 were nominally identical and for the test with reinforcement an attempt was made to measure the deformations of the grid by attaching markers to the nodes of the grid against the side wall of the box. Unfortunately many of these became obscured by clay either during compaction of the fill or during the test; the initial and final positions of those that remained visible are shown in Fig. 14. Whereas with geotextiles there is a tendency for the fabric to pull out from under the fill to either side (Gourc et al 1983), the geogrid is securely anchored by the fill even at such a large displacement of the load. However, as has been observed at a late stage in many of the tests, particularly with the very soft subgrade, there is some tendency for the grid to be pulled down into the clay which is extruded through the apertures of the grid. Movements of the nodes of the grid are predominantly vertical, either up or down, in the area outside the footing; no information has as yet been obtained for the area immediately beneath the footing.

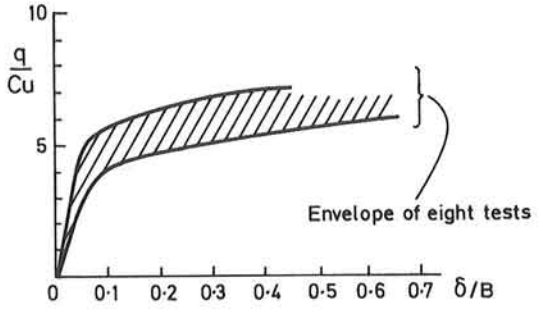

Fig 17. Plot of q/Cu against δ/B for no fill

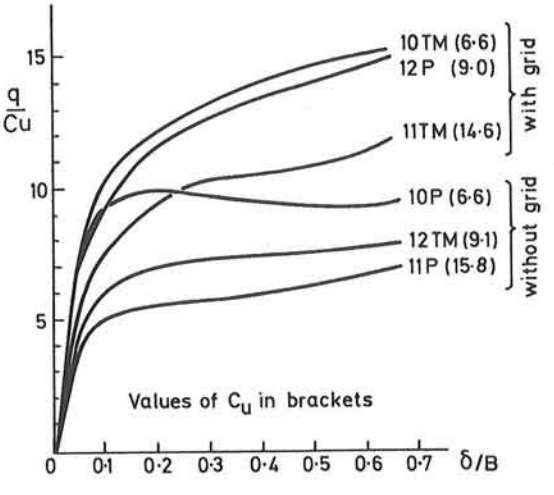

Fig 18. Plot of q/Cu against δ/B for 100mm fill

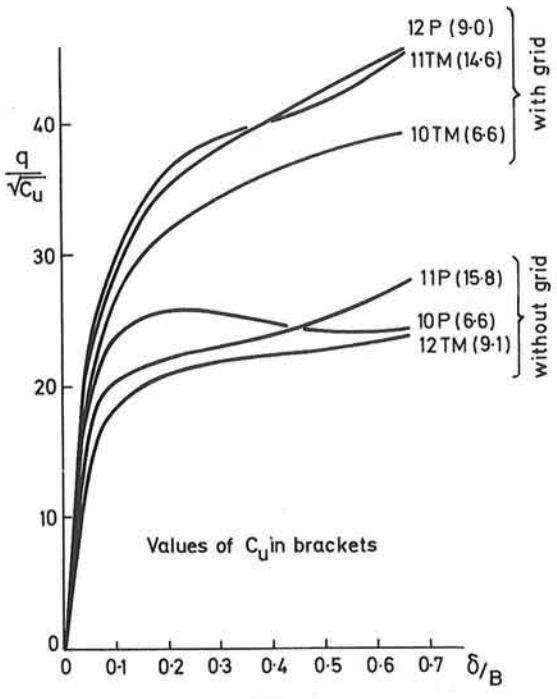

Fig 19. Plot of $q/\sqrt{Cu}$ against δ/B for 100mm fill

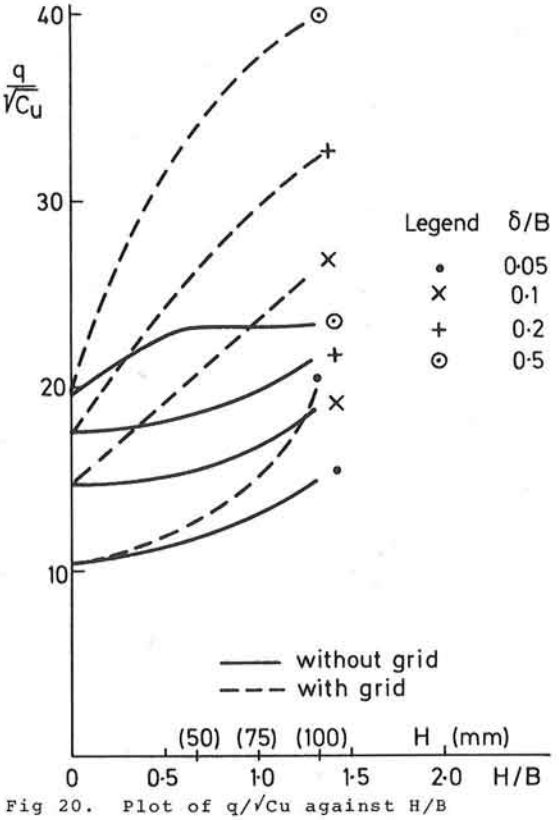

Fig 20. Plot of $q/\sqrt{Cu}$ against H/B

In all cases the volume of heaved clay is equal to the volume of displaced clay to within the possible accuracy of measurement; the clay is therefore deforming throughout at constant volume. The maximum heave at the surface of the fill is monitored throughout each test. Typical results, for tests 12 and 15, are shown in Fig. 15. Heave starts immediately and increases approximately linearly with the descent of the footing. Heave is almost twice as great in the unreinforced system as in the reinforced system, due to the more localised deformations of the whole system and the much greater distortion and hence dilation within the fill. In the field, with repeated loading, such dilation will leave the fill less dense and less able to cope with each successive load application. It is also observed that the effects of side friction on the heave of the fill are much more marked in the tests without reinforcement than in those with reinforcement. This probably happens because the heave in the reinforced system is largely a reflection of the deformations in the clay, which are little affected by side friction, while the heave in the unreinforced system is caused largely by deformations within the fill which are more influenced by side friction.

ANALYSIS

The bearing capacity of a layer of fill overlying soft ground is often considered in terms of the simple model shown in Fig. 16. The angle of load spread α is typically taken to be $\tan^{-1} 0.5$; the coefficient n might be expected to vary with the vertical displacement of the footing δ. Neglecting the initial uniform surcharge of the fill and any forces along the boundaries of the trapezoidal block of fill beneath the footing, the equation of vertical equilibrium is:

$$qB = nCu\ (B+2H\ \tan\alpha) \qquad (1)$$

or

$$\frac{(q)}{(Cu)} = n\ \{1 + 2\frac{H}{B}\ \tan\alpha\} \qquad (2)$$

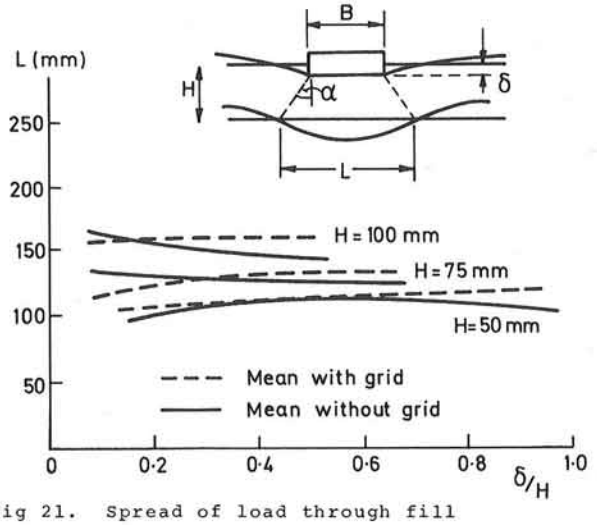

Fig 21. Spread of load through fill

This suggests that, for any particular value of fill thickness H, non-dimensional plots of (q/c_u) against (δ/B) should follow an unique curve, while for any particular value of δ/B (and hence n) there should be a linear relationship between q/c_u and H/B. The latter hypothesis was given some support by results from small-scale preliminary tests using a foam-rubber subgrade (Milligan 1982).

Non-dimensional plots of q/c_u against δ/B for all plots in which the loading was directly onto the subgrade (H=0) are shown in Fig. 17 and give quite close agreement between tests with the full range of c_u used. However similar plots for tests with the thickest fill (100mm) presented in Fig. 18 show a wide scatter for tests both with and without a grid. In each case there is a clear trend, with the curves for the weaker subgrades above those for the stronger subgrades. This suggests that the load-carrying capacity increases less rapidly with c_u than expected. Fig. 19 shows the same results as Fig. 18, only divided by $\sqrt{c_u}$ rather than c_u; the grouping of the curves is now much better though of course the agreement for the results with no layer of fill is then lost. The choice of $\sqrt{c_u}$ is arbitrary and may not be widely applicable to systems with different types of fill, loading, reinforcement etc. The main result of this analysis is probably to show that Equation (2) represents an over-simplification of the performance of a complex system.

Variation of q, again divided by $\sqrt{c_u}$ to minimise the scatter, against H/B is shown in Fig. 20. The superior performance of the reinforced systems is very apparent, the difference increasing with fill thickness and also with footing displacement. Such a plot appears to allow direct comparisons to be made between the performance of reinforced and unreinforced fills of different thicknesses. However, since $q/\sqrt{c_u}$ is not non-dimensional, direct extrapolation to field values of parameters should be done only with great caution. An analytical method is therefore needed which will reproduce the model test results in all major aspects of behaviour and allow extrapolation to field scale with greater confidence. Purely elastic analysis have been found to be quite inadequate to explain the difference in performance of reinforced and unreinforced systems (Milligan 1981). Various attempts have been made to allow for the elastic membrane action of a geotextile in combination with plastic yielding within the subgrade (Giroud & Noiray 1981, Sellmeijer et al 1982, Sowers et al 1982 for example). These generally treat the load-spread angle α as a constant, the same for both reinforced and unreinforced layers of aggregate. However, the experimental results reported above suggest that the greatest benefit from the use of a geogrid is in preventing the lateral spread of fill beneath the load by resisting the tensile strains at the base of the fill. This constraint on the aggregate layer might be expected to allow a much higher effective angle α to occur when a geogrid is being used; an analytical method based on this idea is developed by Giroud et al (1984).

The effective angle α has been determined from the experimental results, α being defined by the points at the fill/subgrade interface which have zero vertical displacement at any stage of a test (see Fig. 21). The appropriate points are probably more correctly the points of inflexion of the subgrade/fill interface, but these are always close to the zero-displacement points and in practice are much more difficult to define precisely. Because the deformations of the system are not always exactly symmetrical and the thickness of the fill varies during a test (particularly in an unreinforced test) it is convenient to define the load-spreading effect by a length L between the points of zero displacement, as shown in Fig. 21. It has been found that L remains practically constant or increases slightly, with α increasing, during the course of a test in which a geogrid is used. When no geogrid is used the value of L for a particular thickness of fill is initially much the same, but reduces during the course of a test, α remaining approximately constant, as shown in Fig. 21. The difference between reinforced and unreinforced systems is somewhat greater for the thicker fills. The back figured values of α at the start of a test vary from about 23° for the thicker fills down to about 19° for the thinner fills. The difference may reflect the greater degree of compaction obtainable in the thicker fills.

Multiplying L by the usual bearing capacity for a clay, 5.14 c_u, gives total loads on the footing which are in general agreement with loads causing initial yield (rapidly increasing displacement) in tests in which a grid was used. This suggests that the membrane effect was negligible, as would be expected at the small displacements of the system at this initial yield stage. For the unreinforced systems, even when the measured values of α (or L) are used, such a simple bearing-capacity analysis greatly over-estimates the allowable loading on the footing; the lateral spreading of the fill beneath the footing must prevent development of the normal type of failure in the clay. Further analysis of the deformation measurements should allow this less safe mechanism to be defined more accurately.

Under normal working conditions the aim should be to maintain loads below the yield load. Even then some rutting would be expected to develop from repeated loading since the deformation will not be entirely recoverable. Limit analyses are not appropriate under such conditions, and work is in progress to model the complete behaviour, but particularly the pre-yield behaviour, using finite element techniques and realistic elasto-plastic soil models. At the same time the laboratory model testing will continue, using dual footings to model a complete vehicle axle and investigating the effects of repeated loading. A larger strong box for this testing is under construction at present. Some simple full scale testing is also envisaged if suitable opportunities arise.

CONCLUSIONS

By simplifying the problem of loading on a layer

of fill on soft ground it has proved possible to identify the essential differences in behaviour between systems with and without a geogrid at the base of the fill, by means of small-scale tests in the laboratory.

The significantly better performance of the systems incorporating a grid has been shown to be the result of the reinforcing action of the grid, which interlocks with the granular fill material and resists tensile strains which develop at the base of the fill. Membrane effects only become significant at large deformations. The bearing capacity of unreinforced fill is less than expected due to lateral spreading of the fill below the loaded area.

ACKNOWLEDGEMENTS

The experimental work reported in this paper was performed by J. P. Love at Oxford University under the supervision of Dr. G. W. E. Milligan. The work is supported by a co-operative award from S.E.R.C. and Netlon Limited. The authors are grateful for many useful comments and criticisms from members of the Steering Committee for the co-operative award, under the Chairmanship of Professor Sir Hugh Ford, and for the assistance of research students, technicians and staff of the Department of Engineering Science, Oxford University.

REFERENCES

Giroud, J. P. and Noiray, L. (1981). Geotextile reinforced unpaved road design. ASCE J. Geotechnical Div., vol 107, No. GT9.

Giroud, J. P., Ah-Line, C. and Bonaparte, R. (1984). Design of unpaved roads and traffiked areas with geogrids. Symposium on Polymer Grid Reinforcement in Civil Engineering. I.C.E. London.

Gourc, J. P., Perrier, H. and Riondy, G. (1983). Unsurfaced roads on soft subgrade: mechanisms of geotextile reinforcement. Proc. 8th European Conf. on Soil Mech. and Found. Eng., (2), 495, Helsinki.

Jewell, R. A., Milligan, G. W. E., Sarsby,R. W., and Dubois, D. (1984). Interaction between soil and geogrids. Symposium on Polymer Grid Reinforcement in Civil Engineering. I.C.E. London.

Milligan, G. W. E. (1981). The use of mesh products to improve the performance of granular fill on soft ground. Report to Netlon Ltd., O.U.E.L. Report No. 1346/81. Dept. Eng. Science, Oxford University.

Milligan, G. W. E. (1982). Some scale model tests to investigate the use of reinforcement to improve the performance of fill on soft soil. Q. J. Eng. Geol. London, Vol. 15, 209-215.

Sellmeijer, J. B., Kenter, C. J. and Van der Berg, C. (1982). Calculation method for a fabric reinforced road. 2nd Int. Conf. on Geotextiles, Las Vegas.

Sowers, G. F., Collins, S. A. and Miller, D. G. (1982). Mechanisms of geotextile-aggregate support in low-cost roads. 2nd Int. Conf. on Geotextiles, Las Vegas.

Wroth, C. P., Randolph, M. F., Houslby, G. T., and Fahy, M. (1979). A review of the engineering properties of soils with particular reference to the shear modulus. C.U.E.D./D - soils TR 75, Dept. of Eng. University of Cambridge.

Stanley Airfield, Falkland Islands, 1982

The paper records the history of events relating to Stanley Airfield, starting with the invasion of the Falkland Islands on 2 April 1982 and leading to the landing of the first RAF Phantom in the following October. To achieve this the airfield had to be strengthened and extended by 2000 ft (610 m) over virgin areas of peaty soil. The paper describes the planning and design work, including the selection of geo-fabrics and grids, the post-surrender reconnaissance and, finally, the airfield construction. The practical aspects of laying the geogrid materials are covered

L. J. Kennedy, *Royal Engineers*

INTRODUCTION

The invasion of the Falkland Islands by the Argentine forces on 2nd April 1982 focussed immediate attention upon Stanley's small airport. The Headquarters of the Engineer-in-Chief (the professional head of the Royal Engineers) soon built up valuable engineer intelligence about the airfield which was provided by Falkland Islanders, resident in or visiting the UK, and others such as the consulting engineers for the original airport project. Messrs Rendel, Palmer and Tritton, who were able to provide their construction drawings and site survey data.

Preliminary studies considered what use the Argentine forces might be able to make of the airport, which provided the only means of conventional air access to the Falklands. It had been built between 1974 and 1976 on the Cape Pembroke peninsula near Stanley to accommodate a weekly feeder service by F27 aircraft of the Argentine military airline, operating from Comodoro Rivadavia in Patagonia, about 600 nm distant. The single runway was 4100 ft (1250 m) long and 150 ft (45 m) wide. It had a design LCN of 16 with a nominal construction of 32 mm of Marshall asphalt and 300 mm of crushed rock. The airport site was known to have a high water table and consist mainly of peat and sand with quartzite rock outcrops. The airport in its pre-invasion state is illustrated at Figure 1.

It was already clear in the early days of the occupation that the Argentines were flying Hercules C130 transport aircraft into Stanley and also lightweight ground attack aircraft such as the Pucara. The important consideration was whether they could develop the airfield to take fast jets such as their Mirage and Skyhawk fighters. The conclusion was that they would need to extend the runway and, from the extended centre-line profile provided by Rendel, Palmer and Tritton, there appeared to be scope for extension without major earthworks. However, knowing the poor ground, it was thought that any extension work would take some months.

After a week or so the airfield problem was starting to be viewed from another direction. Plans were being laid for the re-occupation of the Falklands by our own forces and the use of the airfield by our own aircraft was considered. Evidence indicated that the runway LCN as built was greater than 16, probably nearer 30. Also an extension of 2000 ft (610 m) or more looked feasible. To build an extension at

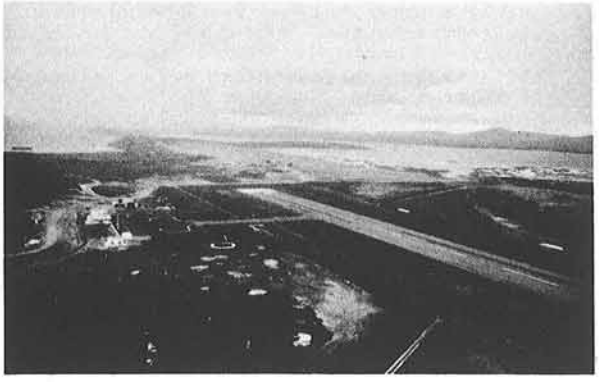

Fig 1. Stanley Airport before April 1982, looking NW.

LCN 30, we examined our range of temporary, rapidly constructed expedients based upon aluminium planks and trackways. Our study intensified when the RAF decided that they needed instead to have a runway of at least LCN 45 capacity, as well as being 6000 ft (1800 m) long. They wanted the ability to operate very heavily laden transport aircraft and fast jets such as Phantom. They also required the enhanced runway in the shortest possible time after the re-taking of the

airfield. Thus we arrived at a firm requirement for developing Stanley airfield.

INITIAL PLANNING AND DESIGN

Clearly, conventional civil engineering options for airfield construction were not possible, because of the time they would take to execute. The only way forward seemed to be by using the aluminium mat expedients already considered. Our airfield mat system, called PSA (prefabricated surfacing aluminium), had been designed to carry Hercules aircraft with low tyre pressures but it was not strong enough for fast jets with high tyre pressures. We had another expedient designated Class 60 Mat, which had been developed as tank trackway and was strong enough. However, we had only limited data on its performance under aircraft loadings and we had never built and operated a full runway system with anchorage and other details established. We were therefore drawn towards the American airfield mat known as AM2. It had the major advantage that it had been designed to carry fighter aircraft with high tyre pressures. Also, it had been developed into a complete airfield package, with accessories for providing adjoining taxiways and parking aprons, airfield lighting and anchorages, and encouragingly it had given proven service in Vietnam. With the strong likelihood of poor ground conditions, the only prudent course was to opt for AM2 Mat even though this would entail a special purchase from the US Government.

Apart from the extension work it was necessary to strengthen the existing runway to LCN 45, and we concluded that a simple over-slabbing of the existing asphalt surface would suffice, assuming of course that any war damage could be adequately repaired.

The initial planning culminated in an intensive weekend in Whitehall when a design team from a unit called Commander Royal Engineers (Airfields) occupied a top floor room in the Old War Office building to make a complete outline plan for the Air Staff for developing the airfield. The planning work included the runway layout, an enlarged parking apron with extra access taxiways, fighter aircraft dispersals, aircraft arrester gears and other support facilities. In conjunction with the staff of the Engineer-in-Chief's department, the plan was phased to permit firstly, the over-slabbing of the existing runway to allow heavy transport aircraft to operate and then, subsequently, the completion of the runway extension and aircraft dispersals to allow fast jets to operate.

Then while the plan was being considered at high level, there was time to review the planning estimates and look at the construction specification in more detail. Without the opportunity for a site investigation (not possible under the circumstances!) we still had to determine with as much accuracy as possible the requirement for engineer plant, equipment and materials, and it was at this time in early May that the intention to use geo-fabrics was examined and selections made.

We were fortunate to have bore hole logs along the general line of the proposed runway extension, provided for us again by Rendel, Palmer and Tritton. An assessment of the engineering characteristics of the soils showed that the main soil types were fine sand and a peaty sand, with the latter type predominant. The extension area was flat, quite level and poorly drained. The water table was very high throughout and there were areas of standing water in places. The peaty sand was forecast to give very low bearing values with a likely CBR of less than 3%.

The conclusion was that we should have a ground membrane such as Netlon CE 121 laid directly upon the subgrade to improve the ground bearing qualities of the soil. It was hoped to avoid cut and lay the geogrid directly upon the undisturbed surface. It was also thought worthwhile to lay a permeable membrane such as Terram under the Netlon to avoid the migration of the peaty subgrade into the selected fill material and reduce any pumping effect during compaction. In the absence of further information we assumed similar conditions elsewhere on the site and made provision for geo-fabric and geogrid materials for the apron extension, aircraft dispersals and access taxiways. We further assumed that we would import beach-won materials to make up levels and provide an adequate base for the AM2 mat.

Time was desperately short with the advance party of the technical team of Royal Engineers needing to catch QE2 leaving Southampton on 12 May 1982. This team was called Commander Royal Engineers (Works) Falkland Islands (or CRE (Works) FI) and the advance party contained a team which would carry out the site survey and site investigation work on the airfield and finalise the design. It was necessary to have this advance party travelling with the second wave of invasion forces to be on hand immediately Stanley was re-taken.

Meanwhile, those left behind carried on the planning, leading to bids for equipment and materials to be shipped south as soon as possible. The Royal Engineer squadrons who would form the construction force started preparing for their deployment.

THE WAR AND THE AFTERMATH

In the South Atlantic the war took its course. The airfield at Stanley received particular attention because, with our Task Force controlling the sea around the Falklands, it provided an aerial lifeline to the occupying forces. There was also the concern that the Argentines would try to base their fast jets at Stanley. Raids by Vulcan bombers and carrier-based Harriers damaged the runway but failed to close it completely.

Immediately Stanley was re-taken the airfield site was reconnoitred. The runway was in an adequate state to land lightly loaded Hercules

doing the short trip from the Argentine mainland but the hasty and poorly executed crater repair work of the Argentines would not be able to carry our own very heavily laden aircraft doing the long trip from Ascension Island. Emergency repairs were put in hand by the Royal Engineer troops who had been operating with the Task Force. We were fortunate to find Argentine supplies of AM2 mat that they had brought to the islands in a vain attempt to extend the runway - they had only laid about 50 ft (15 m) at one end. This matting provided us with excellent crater capping material. We also built a temporary Harrier base alongside the main runway using our PSA aluminium matting mentioned earlier to construct a short runway. This was to permit a continued air defence capability when we had to close the main runway for construction work.

SITE INVESTIGATION

With the emergency work completed, attention was turned to the site reconnaissance for the airfield development project. The first task of course was to clear unexploded bombs and discarded Argentine munitions to permit access to all the site. In general, the desk study layout plan matched the ground quite well. Indeed there were few surprises, with the ground conditions as poor as had been expected. The weather conditions at this time were atrocious. In particular, the constant high winds and frequent blizzards made surveying very difficult. Deep beds of peat were found in some areas and where possible layout adjustments were made. Fortunately in the 2000 ft (610 m) western extension area there was consistently occurring peaty sand.

The water table was high and there was plenty of standing water in the runway extension area. This area was also very flat and level as expected. Figure 2 gives a good idea of the terrain. The main engineering problems were to fix the runway grade line to fit the required criteria while ensuring minimum earthworks, and to provide adequate drainage to the runway area without excessively deep ditches. After much juggling a good arrangement was found.

The major problem to which there was no ready solution was the lack of suitable material for the runway base. With hindsight, our original intention of using beach-won materials seems unrealistic. In the early days the idea of all the likely beaches being sown with mines had not occurred to us. There was plenty of dune sand for general fill but it seemed unlikely to provide an adequate base.

UK TRIALS

While we pondered the runway base problem in the Falklands, a trial at the Aeroplane and Armaments Establishment at Boscombe Down, which tested AM2 laid on ground of varying CBR with multiple passes of an aircraft at the maximum expected all-up-weight, concluded that we should have a minimum CBR of 5% under the mat to avoid unacceptable rutting of the base and mat deformation. It was further deduced that if the sub-grade could not achieve that strength, a base layer of 150 mm of CBR 14% material was required; alternatively a layer of 300 mm of CBR 7% material would suffice. In Stanley, we tested the in-situ CBR of the peaty sand and found it to be in the range 1-3% near the surface. Also, we could not compact the proposed sand fill to achieve a firm surface because of its fine uniform nature. We needed, thus, a base layer to meet the bearing strength requirements of 7 or 14% CBR and there were no naturally occurring materials readily available.

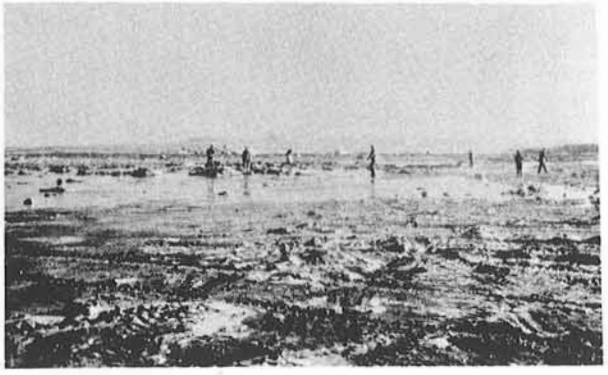

Fig 2. A view of the runway extension site looking W.

A further trial was set up at Boscombe Down to try to find a suitable method of providing a strong enough base. The testing method was as for the first trial but the opportunity was taken to try out a variety of pavement specifications under the AM2 mat. Four sections were prepared in the trial strip. The peaty sand subgrade for all sections was simulated by mixing sedge peat and pit sand. Its CBR was confirmed as 1.5% and a layer of Terram 1000 was laid on top. The first three sections had a further layer of Netlon CE 121 added before the fill was placed. The second section had an extra layer of Netlon CE 121 added at the mid depth of the fill. The third section had the top 150 mm of sand fill stabilised with 8% cement. The fourth section without the Netlon CE 121 was also stabilised. The pavement was topped with an impermeable membrane and the AM2 mat. The mat was trafficked by heavy aircraft and settlements measured.

The two unstabilised sections failed to provide adequate bearing though the second section with Netlon CE 121 at mid-depth (225 mm deep) was significantly stronger. The two stabilised sections showed no distress and there were no measurable differences to reflect on the omission of Netlon CE 121 at the subgrade level.

There were many useful lessons to come out of this trial. Cement stabilisation was a possible solution to the mat base requirement. In deep sand fill the Netlon CE 121 geo-grid

seemed to have a stiffening effect and it was recommended for inclusion in the slopes of any deep sand fill embankments. The Netlon/Terram sandwich laid directly on the subgrade was recommended, especially in view of the poorer drainage conditions to be expected at Stanley. The problem was recognised of Netlon 'bow-waving' or opening at the joints when laid upon an uneven surface or when fill was hastily dumped without care.

FINAL DESIGN

The second Boscombe Down trial was followed by a trial of cement stabilisation on site at Stanley. Here, the stabilised layer did not gain any strength and would not compact in the top 50 mm or so. We concluded that the most likely cause of failure was the extremely poor weather with the temperatures hovering around freezing for much of the time. The other option for providing an acceptable foundation for the airfield mat was to manufacture crushed rock for the base layer. Equipment was already being provided to establish a quarry for concreting aggregates and road stone but the extra need for large quantities of crushed rock for the mat base was a daunting prospect. There was, though, no other choice.

The final design for the runway pavement, outside the extent of the existing runway, is illustrated in Figure 3. The subgrade was to be the undisturbed ground wherever possible. The addition of Tensar SS1 at the interface between the sand fill and the rock base was a later addition during construction when it was found that stone was being lost in the sand during compaction. The basic requirement for the runway surface level was 1 inch in 12 feet (25 mm in 3.66 m). The rock layer was to be covered with an impermeable membrane called 'Trevira', to prevent water percolating through the mat joints and penetrating the base and weakening it. Finally the AM2 mat was to be laid on top. (The mat consists of interlocking panels measuring 12 feet by 2 ft by $1\frac{1}{2}$ inch thick (3.66 m by 0.6 m by 38 mm), that are laid in a bonded pattern across the runway, the short dimension being parallel with the runway centre line. Each panel weighs 144 lb (65 kg)). The specification for deep fill embankments was as recommended from the UK and this is illustrated in Figure 4.

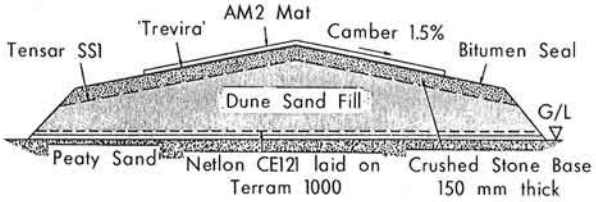

Fig 3. Cross section through runway extension.

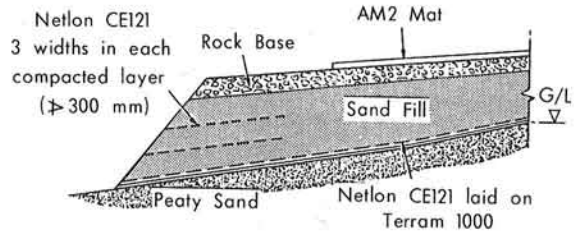

Fig 4. Cross section through embankment.

CONSTRUCTION

Even while the war continued, the stores and equipment for the airfield project were being gathered together for shipment, including 4000 tonnes of AM2 matting that was shipped from the United States to the UK prior to being incorporated with the rest of the stores. Certainly there was no question of our site reconnaissance having any effect on what we were being provided with to execute the work (it was an unusual situation to say the least!). Of course a small number of urgent items of equipment could be flown in on the 'air-bridge' via Ascension Island but, in general, we had to plan our task to suit what was already coming down to us by sea.

By mid July, just over a month after the surrender, the two shiploads of stores plus two fresh squadrons of Royal Engineers had arrived in Stanley. CRE (Works) staff were still working against the clock producing the working drawings and specification for the works. The construction force concentrated initially on getting the stores ashore and establishing a quarry. The stores unloading was a major task because Stanley possesses no deep water port facility. The stores ships were obliged to anchor in Port William outside Stanley Harbour and rafts (made up from 'Mexeflote' pontoon sections) and powered lighters operated to slipways constructed by the Royal Engineers. There were over 9000 tonnes of cargo for the airfield to be moved in this way including some very heavy items such as rock crushers (the primary crusher units weighed 45 tonnes). The unloading process took about three weeks.

The initial work on site covered drainage and the aircraft arrester gear foundations: these were massive concrete foundations founded at a depth of 2.2 m in running sand. Fortunately we had included well pointing kit in our equipment package; without it this task would have been impossible. The next stage was to overslab the existing runway with the AM2 mat. This involved more substantial repairs to the cratered areas and a re-shaping at each end of the runway to accommodate the vertical curves in the longitudinal profile joining into the proposed runway extensions. The AM2 mat was laid with a very large number of men working

3 hour shifts with 9 hours off. Handling the heavy mat panels in the high winds and at very low temperatures was an arduous task and 3 hours at a time was as much as could be managed. The runway closure was for 12 days in late August. Then the 4100 ft (1250 m) length of overslabbed runway was put back into use. During the closure, air defence cover was provided by the Harriers.

Attention then turned to the runway extension and other areas of new construction. By then it was September, spring was around the corner and the ground conditions became marginally better. Some levelling work was needed on the subgrade and a few bomb craters in this area needed filling. The digging of decent drainage ditches also caused a marked improvement in the ground conditions. The Terram and Netlon CE 121 went down very easily and proved an excellent platform for the subsequent filling work. The only difficulty with the Netlon was the tendency of it to wrinkle and gape at the overlap joints when fill was placed on top. Fortunately we had had plastic ties sent out to us on the airbridge and these cured the problem. The recommended spacing for the ties was 1.5 m but we found it better to reduce the spacing to about 0.6 m. Figure 5 shows the Terram and Netlon CE 121 in use.

The dune sand fill was placed if required or else the crushed rock base went down straight upon the Netlon. We found it essential to have at least 200 mm of loose material on top of the geogrid when doing rough grading. Otherwise the grid caught on blade corners and was ripped. The stone layer did then usually exceed the 150 mm requirement, though after compaction it was of course closer to that thickness. About half the runway extension length required sand fill.

In the strong winds and generally drying conditions in September it was impossible to retain sufficient moisture in the sand for optimum compaction. Its consistency soon resembled that of dry salt and it was impossible to stabilise the top surface. The Tensar layer that we introduced proved very useful as a separation layer between the sand and the stone and it also of course provided more shear strength. The Tensar layer is shown in Figure 6.

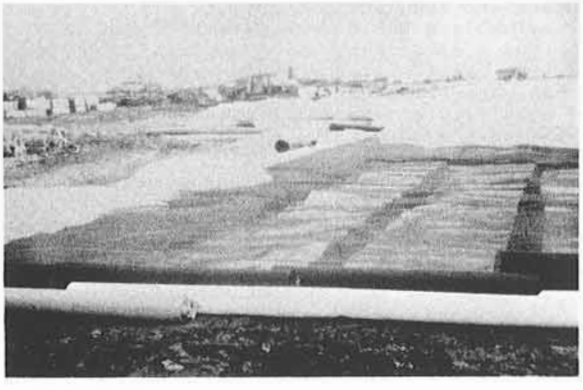

Fig 5. Terram and Netlon CE 121 on subgrade.

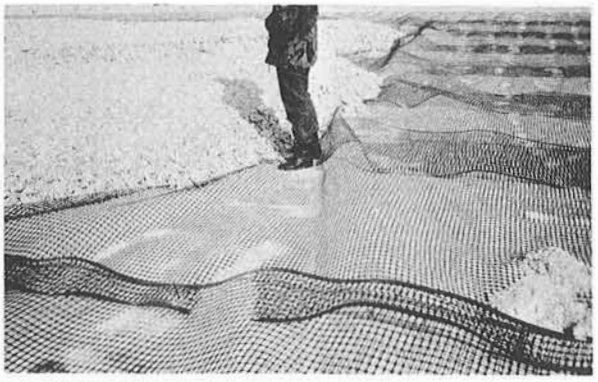

Fig 6. Tensar SS1 used as separation layer.

The crushed stone production became the most critical activity of all. The decision forced upon us to found the new pavement areas upon a graded stone base led to a requirement for tens of thousands of tons of crushed rock. We had early problems with our rock drills. They were too lightweight and insufficient for the production rate required. Fortunately we were able to fly in more drills of a heavier variety. The critical equipment then became the rock crushers. It was as well that we had 2 sets of primary and secondary crushers, our suppliers had wisely provided at least two of everything where possible, and both sets were put to work. Still we had many difficulties. In part these were due to the very hard nature of the quartzite rock which caused crusher jaws in particular to wear very quickly. The other limitation was our own experience but we learnt fast and benefited from a number of technical advisory visits.

We started off with a specified grading for the base rock of a 40 mm graded layer topped by a 20 mm aggregate. In practice this was greatly modified. The secondary crusher could produce 40 mm stone but the penalty was excessive jaw wear. We settled in the end for a 100 mm down crusher run material topped with the 40 mm down fraction that we had to screen in a secondary operation. Further refinements were impossible if we were to meet the 1000 tons per day requirement. Our base strength requirement of CBR 14% was of course assured using crushed rock but we needed to achieve adequate compaction and a smooth grade to accommodate the AM2 mat. This we managed even with the large sizes of rock used.

In fact we achieved a very hard concrete-like surface upon which we rolled out the 'Trevira' material. We had selected this material from a sample sent to show the cladding material for the prefabricated aircraft shelters made by Rubb. We had been worried about the durability of the membrane sandwiched between the crushed rock and the metal mat which we knew would

move under aircraft loadings. The very tough Trevira, though designed for building use, satisfied our requirement.

The AM2 mat laying was relatively straightforward and a less critical activity when only required to keep pace with the completion of the base layer. The second phase of the development work included the 2000 ft (610 m) runway extension, one aircraft dispersal area and a number of aircraft arrester gears and it was completed in time for the arrival of the first Phantom aircraft on 17 October 1982. The second phase of the work had taken 6 weeks and the overall task had taken about 2 months from the time the stores had been assembled on site. The time from the initial conception in London had been a little over 6 months. A view of the completed runway is shown at Figure 7.

Fig 7. Runway looking E with extension in foreground.

ROAD CONSTRUCTION

We also built many roads around the airfield site. Our early experience led us to use our geofabrics and geogrids for these too. Various combinations were tried until we arrived at our most economical and effective solution which is illustrated in Figure 8. We generally found 200 mm of crushed rock an adequate surfacing layer but later on, when putting in haul roads for the dump trucks carrying rock fill to other sites, we found it necessary to increase this layer to 300 mm. We found Netlon CE 121 perfectly satisfactory as a geogrid for roads but eventually opted for Tensar because it was lighter and cheaper and did the job just as well.

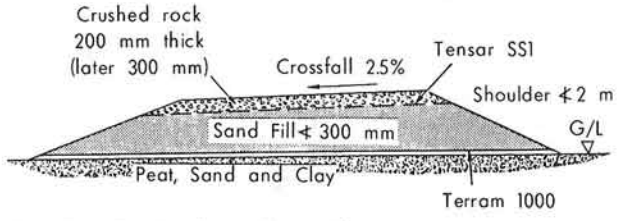

Fig 8. Typical road section

CONCLUSIONS

It is not possible to put a precise value on the geofabrics and geogrids used in the development of Stanley airfield. In the emergency context, preliminary site trials were not possible. The design was based upon engineering commonsense (a subjective view!) and a prudent wish to use any means readily available to avoid pavement failure. We were not so constrained by financial limits but had an absolute need to guarantee results. It is difficult to assess the engineering risks taken and, at the time, there was little opportunity to dwell upon them. Also, the eventual base for the airfield mat was so strong that localised failure in the pavement was unlikely. It is worth then considering the longer term performance where inadequacies and more general failure might become apparent.

In fact the airfield has performed very well The maintenance problems have nearly all been related to the AM2 mat as a result of movements induced by aircraft. One failure of the base, shown by rutting along the Hercules wheel tracks in one section of the runway, was caused by the dislodgement of the Trevira membrane caused by the AM2 mat rocking across the runway crown and pulling the membrane by suction. This caused gaps for surface water to percolate through and led to localised weakening of the base; the base did not actually fail, as it was still necessary to attack it with picks to carry out repairs. The solution to the membrane problem was to place a layer of Netlon CE 121 between the mat and the membrane and this effectively broke the suction.

There has been some general settlement in areas of fill. The likely causes here are settlement in the sand fill which was compacted to a reduced standard when we could not maintain a high enough moisture content and, secondly, settlement of the subgrade following the drainage of the area.

We are left then with the conclusions that for the airfield pavement works the use of geogrids provided a sound base for the placing and compaction of the sand fill and crushed rock layers, provided a positive separation layer between the sand and the rock to save waste of the valuable crushed rock material, and provided a novel separation membrane under the AM2 mat itself. Also the geogrids most probably contributed to the overall strength and stability of the whole pavement system. As far as the road works are concerned we have more positive evidence that the geogrids were essential components in providing adequate roads without the excessive use of hard-won natural materials. We can only remain thankful that the failure limit for the runway itself was not demonstrated at Stanley in 1982.

Geogrid applications in the construction of oilfield drilling pads and access areas in muskeg regions of Northern Alberta

Gulf Canada Resources Incorporated uses Tensar polymer geogrids as a muskeg stabilizing agent for access road and drilling pad construction over muskeg areas in Northern Alberta. Drilling operations can last from 40 to 60 days and if the well goes into production the site may be in use indefinitely. Various techniques of subgrade preparation are discussed. Different design parameters including grid orientation, fill quality and supply are considered, to accommodate expected dynamic and static load conditions. The Tensar geogrid and fill system is evaluated in terms of overall settlement and reaction to static and dynamic loads over time. A comparison of geogrids to commonly used stabilizing agents and construction techniques is addressed.

J. B. Kroshus and B. E. Varcoe, *Gulf Canada Resources Inc.*

INTRODUCTION

During 1982-83, G.C.R.I. drilled 270 wells in Western Canada, approximately 8% of these were on muskeg. The Exploration and Development program for 1983-84 will increase the number of muskeg locations fourfold.

The purpose of this report is to illustrate the effectiveness of Tensar geogrids in providing stable soil conditions for short term drilling and production operations on muskeg locations.

DISCUSSION

Characteristics of Northern Alberta Muskeg

"Muskeg" is the term used to describe organic terrain containing a peat structure with an associated vegetation cover and related mineral sublayer (MacFarlane, 1969).

In Northern Alberta, the vegatation cover encountered is generally a Class A or Class B (trees from 1.5m - 4m). The subsoil varies from ablation tills to clay and is difficult to characterize.

The peat structures vary from fine fibrous to coarse fibrous with depths of 10cm to 10m.

Water content ranges from 50% to 760% and shear strengths vary from 2 kPa to 29 kPa.

DESCRIPTION OF LOADS

The major static loads applied to the drilling rig matting are the weight of the rotating equipment, mast, blocks, substructure, mud tanks and tubulars. The bearing stress below the matting* is relatively low (peak bearing stress = 30 kPa, average = 15 kPa). Our concern during drilling is not one of overall consolidation but rather that of differential settlement which would require jacking of the rig substructure or drillpipe storage racks.

*Assuming a 3600m drilling rig (well depth rarely exceeds 3500m in Northern Alberta muskeg regions).

The important static loads are: *

		WEIGHT (kN)	BEARING PRESSURE (kPa)
1.	Rotating equipment, mast, block, substructure and drillpipe (applied through matting)	3400	30
2.	Fully loaded pipe racks	980	150
3.	Water tank	620	100
4.	Cement tank	380	90
5.	Mud Tanks	710	15
6.	Overlying fill material (based on 1 m layer @ 20 kN/m^3)		20

The traffic patterns on the lease (See Figure 1) impart more critical shear and bearing stresses to the surface. The greatest dynamic load is the transport of the drawworks (approximately 450 kN) on a tandem-tandem tractor trailer truck.

Typically, the dynamic loads are:

OPERATION	VEHICLE TYPE	AVERAGE LOAD (kN)	FREQUENCY (cycles)
Move in	Tandem Truck	220	25
Drilling	Vacuum Truck	220	160 - 240
	Cement Bulkers	400	3
	Cement Trucks	220	4
	Casing Trucks	400	15
	Pick-up Truck	10	200 - 300
	Miscellaneous	30	12 - 16
Move Out	Tandem Truck	220	25

Assuming a drilling duration of 40 -60 days.

FIGURE 1

RIG LAYOUT AND TRAFFIC PATTERNS

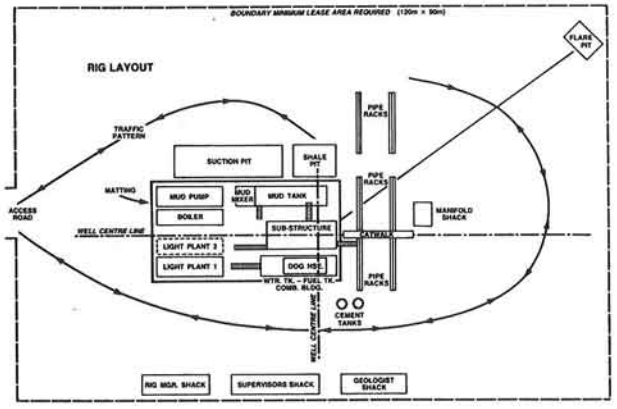

CASE HISTORIES

A. Drilling pad construction using Tensar AR1

Location: Sturgeon Lake, Alberta
Date: August 1982

Site Details:

1. Lease Area = 9,300m^2
2. Condition of Lease = Drying after heavy rains
3. Depth of peat = 1.0m
   Water content = 350%
   Undrained shear strength = 5 kPa
4. Subsoil = 1.5m of sandy clay overlying rounded gravel
5. Maximum static bearing pressure = 150 kPa
6. Maximum dynamic load = 450 kN

The decision to use geotechnical reinforcement was motivated by a severe construction time constraint aggravated by wet weather. Tensar AR1 was chosen because of its competitive initial testing price and G.C.R.I.'s belief that Tensar was a better product than conventional geotextiles.

Construction:

The site had been levelled of brush and trees which were laid directly over the muskeg. The geogrid was unrolled perpendicular to the anticipated rig traffic with a grid overlap of 200mm along the length and 2m at the ends.

A low plastic fill material (40% sand, 60% clay) was applied as a 1m expanding wavefront. This "Rolling Surcharge" method of fill placement was used to reduce slack in the geogrid sheets and squeeze some of the water from the peat in an attempt to reduce future subsidence of the pad. Fill compaction was achieved using a sheep's foot compactor. The average height of fill at the end of construction was 880mm.

Observations:

With straight clay fill and no geotechnical reinforcement, the larger fill lumps punch through the muskeg root mat resulting in more material being used. With Tensar geogrids, there was a more uniform bearing pressure applied to the root mat and its integrity was maintained.

A calculation done by Pavement Management Systems Consultants predicted the maximum tensile force in the geogrid to be 12 kN/m, well below the biaxial tensile strength of Tensar AR1 (21 kn).

The lease responded well to rain and rig traffic. No surface deformation was encountered and the average overall pad consolidation at completion of the drilling operation was found to be approximately 215mm.

Based on our construction and maintenance experience, geogrids provided quicker access to the location. Very few maintenance problems were encountered and pad subsidence was minimal. The pad was constructed in 5 days compared to 8 days for an adjacent lease (no geotechnical reinforcement and 1.25m of fill), thereby saving approximately 14% in construction costs.

CASE HISTORIES

B. A comparative study of Tensar SS1 and a heat-bonded geotextile for muskeg reinforcement during production operations.

Location: Pelican Lake, Alberta
Date: January 13, 1983

Site Details:

1. Lease Area = 10,800m^2
2. Condition of Lease before construction = 1.0m of frost penetration
3. Depth of peat = 1 - 1.5m (deepening at the north end)
   *Water content = 50 - 200%
   *Undrained shear strength = 5 - 20 kPa
4. *Subsoil
   - 3 - 5m of low to medium plastic ablation till (penetration from 72 to 432% kPa)
   - 1.2m of sand
   - basal till (penetration readings 432= kPa underlies the sand and ablation till)
5. Maximum dynamic load = 250 kN (Tanker truck)

Construction:

Trees on the lease were levelled and the site divided into 3 north-south strips. The central strip was excavated to the mineral sublayer (removing an average of 1.3m of muskeg) and refilled with sandy clay. The geotextile was laid longitudinally on the muskeg west of the clay section and the geogrid was laid longitudinally to the east.

The entire lease was then backfilled with 1.0m of clay and sandy gravel. Compaction was very limited consisting mainly of D6 caterpillar traffic.

Observations:

Settlement data (Fig. 2) was obtained over the following year for each of the three lease strips. As expected the settlement of the clay strip (all muskeg removed) was less than the two strips where the highly compressible muskeg was not removed. Of the two muskeg strips, the performance of the Tensar geogrid strip was superior to that of the geotextile strip. Comparison of the two strips between April and August 1983, shows that on the south side of the site, settlement of the geotextile strip was 2½ times greater than settlement of the geogrid strip. On the north side of the lease where the depth of muskeg is greater, the settlement of the geotextile section was 38% greater.

From these results it can be concluded that total settlement can be minimized by removing the muskeg and replacing it with fill. This can only be achieved if the muskeg depth is shallow and replacement fill is economically available. At the Pelican Lake site, the muskeg varied from 1.0m - 1.5m, and the cost of fill was very low due to its proximity to the site. For this set of conditions, the muskeg removal and fill replacement alternative was 24% less expensive than the reinforced pad alternatives. Where the above cited conditions are not met, however, geogrid reinforcement has been shown to be cost effective and has achieved superior performance over the geotextile reinforcement used in this study.

*Taken from soils report describing the Pelican Lake Area.

A 142m^3 oil storage tank located on the geotextile/clay interface developed a severe list towards the geotextile section (after 4 months) and consequently was repositioned on the clay surface.

Visual inspection indicated the geotextile section was prone to rutting. (After 6 months heavy traffic avoided the area). Minimal rutting was encountered on the geogrid and clay sections.

FIG. 2
RELATIVE SETTLEMENT OF PELICAN LAKE DRILLING PAD
(11-5-81-22 W4)

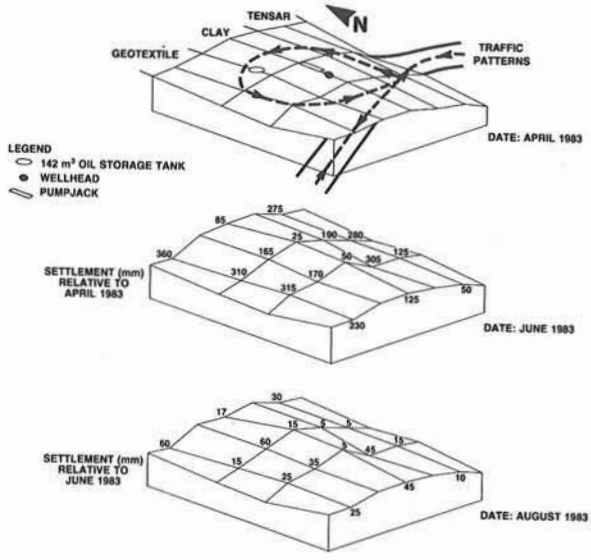

CONCLUSIONS

1. Tensar geogrids have proven economical and effective in stabilizing muskeg for summer construction of drilling pads and access roads. They have proven effective in maintaining surface integrity of the pad during drilling operations. Fill cost and muskeg depth are the major factors in determining the economics of geogrid application. The observation period has not been long enough to quantify maintenance savings.

2. Without a major clay constituent, sandy fill (due to its low shear strength) is unacceptable as a traffic surface. Tensar geogrids (when placed at the muskeg/fill interface) have a very limited effect on providing surface stability (reducing surface rutting). Surface stability can be improved by placing a second layer of geogrid reinforcement at a shallower depth.

3. The "Rolling Surcharge" method of fill placement has been effective in reducing the future compressibility of muskeg by driving water away from the structure and preventing slack in the Tensar sheets.

RECOMMENDATIONS

1. When drilling pads and access roads are built on unfrozen muskeg, the bulk of settlement occurs during and shortly after construction, thereby allowing the surface of the fill to be properly graded prior to putting the pad or road into service. If these structures are built over frozen muskeg, the bulk of the settlement occurs shortly after the subsequent spring thaw. Although Tensar geogrids are effective in reducing the differential nature of spring thaw settlement, the presence of reinforcing will not prevent total settlement from occurring. However, where geogrids are used to reduce the thickness of fill required, settlements are reduced because the total weight of fill is reduced.

2. Winter leases on muskeg should be constructed with a minimal amount of fill to take advantage of support provided by frost penetration. If the well goes into production, a layer of geogrid and more fill should be added after the first major thaw to stiffen the surface and compensate for the thaw consolidation.

3. Care must be taken not to puncture the root mat when preparing a muskeg location for construction. Levelling the trees on muskeg provides the most stable base for Tensar geogrid application.

4. A market potential for Tensar geogrids of several million dollars exists for the 1983-84 drilling season. In order to utilize the product more effectively, G.C.R.I. suggests that design curves be established to optimize the use of this reinforcing material in muskeg with a variety of fill materials.

REFERENCES

1. MacFarlane I. (1969), Muskeg Engineering Handbook. 1-130, University of Toronto Press. Toronto, Ontario.

Evaluation of geogrids for construction of roadways over muskeg

Large scale plane strain loading tests have been made on gravel fills compacted on a peat subgrade. The fills were tested with and without Tensar geogrid reinforcement. Detailed measurements were made, of the deformed shape of the geogrid, of tensile loads in the geogrid and of geogrid movements under load. The results are being used to develop simple design methods for geogrid reinforcement of expedient roads and to assist development of comprehension of the mechanics of behaviour in geogrid reinforced soils.

P. M. Jarrett, *Royal Military College of Canada*

INTRODUCTION

The organic soils and peats, which form the surficial layers of muskeg or peatlands, represent a formidable obstacle to the road-builder and to those wishing to establish temporary or permanent earth structures on such deposits. The basic problems in such construction lie with the extremely compressible nature of virtually all peats and organic soils and in cases of well decomposed organic soils with their low shear resistance.

In many situations, roads and railways have been constructed over deep muskegs using the tensile resistance of the natural surface mat as a primary supporting mechanism. Such surface mats are formed from interwoven roots and other plant remains. The use of corduroy construction, in which a continuous bed of logs is formed beneath the road, is also common in such circumstances. It is, therefore, not surprising that geogrids represent a potentially valuable aid as a tensile reinforcement in earthworks constructed over peats. Geogrids possess a more uniform and predictable tensile resistance than a natural surface mat and would be easier to use in construction than a full corduroy roadbed.

The tests reported in this paper are an attempt to quantify the benefits of Tensar geogrids in such construction and to allow a better understanding of the mechanisms involved in their use as a tensile reinforcement in soils.

TESTING APPARATUS

Large scale plane strain loading tests have been made in the laboratory on a series of compacted gravel fills, constructed on a 1 m deep peat subgrade. The tests were carried out in a test pit which is 3.7 m long by 2.4 m wide and 2 m deep. Loading was applied to the compacted gravel surface through a 203 mm wide beam spanning the full width of the test pit. The load was generated using a computer-controlled MTS hydraulic actuator. The test pit is shown during operation in Plate 1.

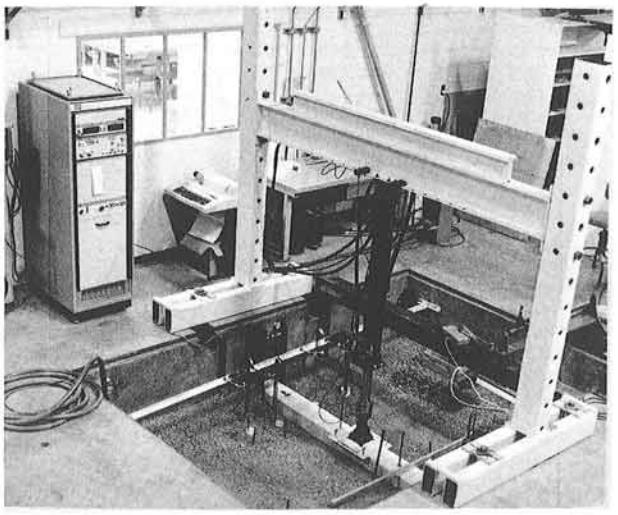

Plate 1
Test Pit Arrangement

The peat subgrade was formed using bales of air dried, finely fibrous, horticultural sphagnum peat with a low degree of decomposition. Water and peat were mixed in the test pit to a depth of about 1.3 m after which excess water was drawn out of the mixture using a series of drain pipes on the floor of the pit.

This downward drainage consolidated the peat to a thickness of 1.0 m with the following typical average properties:

Moisture content - 850%

Vane shear resistance - 4 kN/m^2

After each test, the peat was loosened by digging, water was then added to bring the volume back to the 1.3 m depth and compressed air was bubbled through the system to complete dispersion of the peat-water mixture. After the dispersion, the peat was reconsolidated using downward drainage to provide the subgrade for the next test.

Gravel fills 305 mm thick were compacted on the peat subgrade in two lifts using a Wacker vibrating plate compactor. The nominally 20 mm gravel was formed from crushed limestone with the following gradation:

100 % passed 20 mm
50 % passed 10 mm
22 % passed #4 Sieve
9 % passed #10 Sieve
4 % passed #20 Sieve
1 % Fines

Compacted dry densities were in the order of 1920 kg/m^3 at a moisture content of 1.8%. Fills were compacted with and without geogrid reinforcement. In the reinforced cases the Tensar Geogrid Type SS2 was placed at the peat to gravel interface.

The following monitoring procedures were used when appropriate:

1. The load applied and the displacement of the actuator piston were monitored through built-in transducers and the computer controlled data acquisition system.

2. Cross checking of the beam displacement with the movement of the actuator was carried out using dial gauges reading directly onto the beam.

3. Vertical movements at the peat-gravel interface were measured at various distances from the beam centerline. This was achieved primarily using settlement plates at the interface with attached rods passing through the gravel so that a series of level readings could be taken as displacement occurred.

4. Horizontal movements of points on the geogrid were observed. To do this, small plywood boxes were inserted into the gravel exposing a section of geogrid. Travelling microscopes were then used to sight on a fiducial mark scratched on a geogrid junction point.

5. Load cells were manufactured which could be inserted as a joint in a 305 mm wide strip of geogrid. The cells transmitted the tensile load between sections of the geogrid strip through 8 Aluminum fingers. Each finger had 2 electrical resistance strain gauges attached to it. The strain gauge readings were calibrated against tensile load. Three such cells were inserted in one strip of Tensar. They measured tensile loads directly beneath the loading beam and at distances of 400 mm and 800 mm from the beam centerline. The instrumented strip was placed along the longitudinal centerline of the pit and as plane strain conditions prevailed this should not have influenced test behaviour.

TESTING PROCEDURE

In order to simplify analysis, an incremental static loading procedure was adopted. Each load level was applied to the beam until the rate of displacement became less than 0.02 mm/min. At this time, the load was increased unless it occurred at a time when the test operator was not present. In this case, the increment would be applied as soon as he returned and made the necessary manual readings of the settlement plates and travelling microscopes. Loads were increased until at least 200 mm of beam displacement had occurred. At this point, a series of 5 unload-reload cycles were performed. The load on the beam was reduced to 2.5 kN for 100 minutes and then increased to its previous maximum for 100 minutes. This represented one cycle. At the end of the cycling the beam was completely unloaded, removed and the rut formed by the test, filled by the addition of compacted gravel. The beam was then replaced and reloaded in increments to the previous maximum, after which a further series of unload-load cycles was instituted. Following these cycles, incremental loading was continued to higher levels. At the maximum load level further unload-load cycles were also carried out. The complete beam load against beam displacement results are given for a Tensar reinforced test in Figure 1. This test was repeated twice with virtually identical results.

The procedure for testing the unreinforced fill was similar in the initial phase. However, the load increment which took the beam beyond 200 mm of displacement had to be terminated, because the rate of displacement did not fall to the required value. As the system was showing signs of distress with a punching failure in progress, the cyclic loading was not performed. The rut was, however, filled and the beam incrementally reloaded. After the load was increased and again showed signs of failure, a series of unload-load cycles were carried out. The beam load-beam displacement results from this test are given in Figure 2, where they may be compared with an abbreviated form of the reinforced test.

In addition, beam load tests were performed directly on the surface of the peat as a measure of its compressibility characteristics. The rate of displacement criteria was the same in these as in the other tests. Displacements

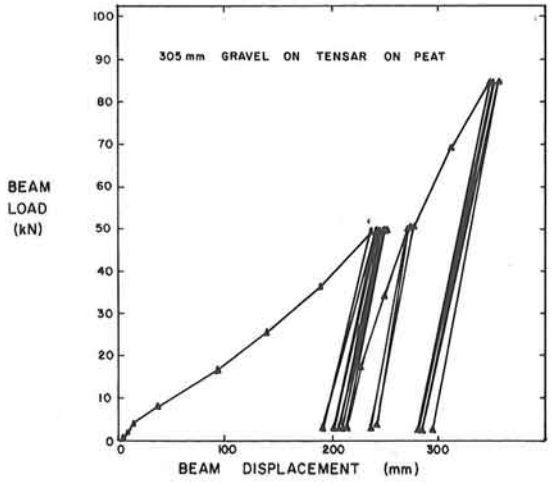

Figure 1
Beam loading results for reinforced fills

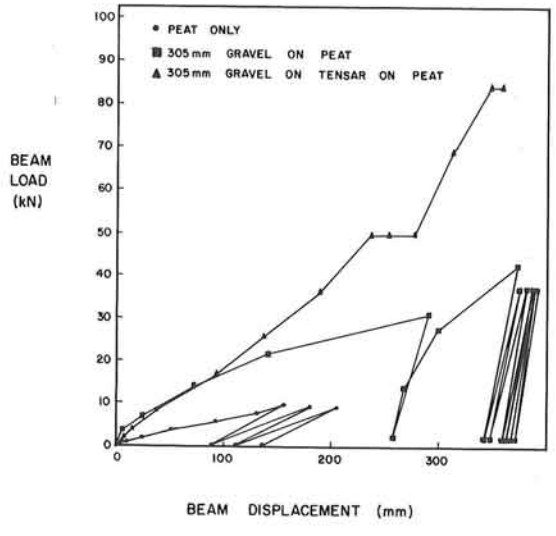

Figure 2
Beam loading results for all tests

could not be taken so far in these tests as the beam and foot of the actuator were disappearing beneath the water table into the peat. The results for these tests are also given in Figure 2.

DISCUSSION OF BEAM LOAD-BEAM DISPLACEMENT RESULTS

The unreinforced fill appeared to be in a state of distress under the application of the 31 kN load level, as its rate of displacement did not appear to be decreasing to the required level. On the other hand, the geogrid reinforced fill took over 50 percent more load without undue distress and also withstood the load-cycling procedure.

The decision to fill the ruts after 200 mm of displacement was arrived at in relation to the probable maximum rut depth allowable in a temporary haul road. It may be seen that after filling the ruts loads were increased to 85 kN and this produced only 120 mm of new displacement. This form of result gives credence to the procedure of producing a rutted fill during construction and then filling the ruts prior to use.

At the start of the tests it may be seen that no difference between the unreinforced and reinforced cases was measured until close to 100 mm of displacement had occurred. This is a common finding in such studies and indicates that the reinforcement is acting in this situation primarily as a stretched membrane. It is possible, therefore, to use developments of the types of analysis suggested by Giroud and Noiray (1981) and Sowers, Collins and Miller (1982) to assess the tensile loads carried by the geogrid. The only major difference between the peat problem and the clay problems dealt with by the quoted authors is that peat represents a drained situation, where constancy of volume cannot be assumed. However, using the results from the three forms of tests shown in Figure 2 and the procedures outlined by Jarrett (1983), estimations may be made of the relative contributions of the peat, of the gravel and of the geogrid to the overall bearing capacity. From these results and the deformed shape of the membrane calculations of the tensile forces in the geogrid can be made.

TENSILE LOAD MEASUREMENTS

The load cells in the Tensar strip were used in one of the two reinforced tests and functioned well. The results obtained are summarized in Figure 3 for Cell 1, which lay directly beneath the centerline of the beam and in Figure 4 for Cells 2 and 3, which lay respectively 400 mm and 800 mm from the centerline. The loads have been presented in terms of kilonewtons per meter for convenience of reference.

Considering Figure 3, tensile forces of approximately 10.8 kN/m were generated under a beam load of 48 kN. During load cycling some

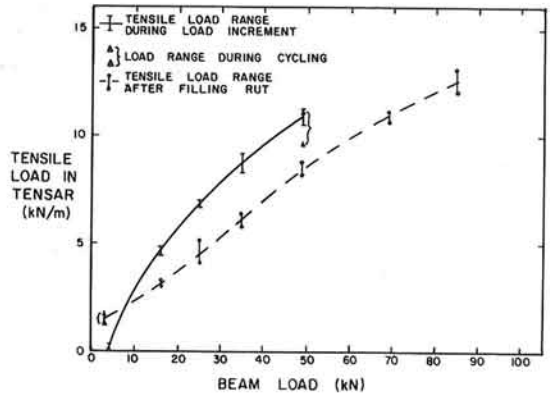

Figure 3
Tensile loads measured in Cell 1 on beam centerline

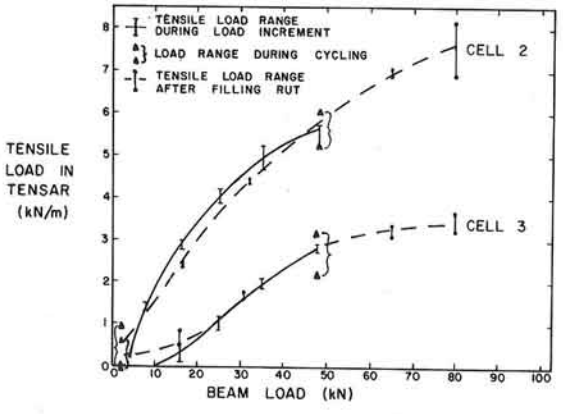

Figure 4
Tensile loads measured in Cells 2 and 3

tensile force remained locked into the system in the unloaded phase and very consistent values of tension were measured over all 5 cycles. After the rut was filled application of the same beam load produced smaller tensions in the geogrid. This is presumed to be due to the better load spreading caused by the thicker gravel layer. In fact, the maximum tension reached only increased to 12.5 kN/m under application of the higher load levels. This, it is felt, was due partly to limitations in the lateral anchorage of the geogrid that may be better explained after study of Figure 4.

Cell 2 lay 400 mm from the centerline and coincided with the inflexion point in the curvature of the geogrid from concave beneath the beam to convex towards the outside. At this point the effect of the geogrid changes from decreasing the load on the subgrade beneath the beam to increasing it as the load is spread laterally. The difference between the tensile force before and after filling the rut was much smaller at this load cell. Little extra gravel was added this far from the centerline and so the tensile behaviour remained the same.

At Cell 3 little vertical movement was measured and so the tensile force was being applied virtually horizontally. This means that this cell is in an anchorage zone. The facts that the tensile force appeared to reach a maximum and that the travelling microscope readings showed the Tensar to be slipping towards the centerline indicate a limitation in the testing arrangement. In essence, the geogrid is not reaching its full tensile capacity because of an insufficient anchorage length.

This may have practical implications as the geogrid does extend 1.85 m laterally from the centerline of the load. This may well be a greater distance than is usually provided outside the wheel paths on a single track haul road.

Despite the absolute limitations of the anchorage, valuable information is available from these results on the mechanism of geogrid anchorage. This point can be more fully developed when the tensile loads measured in Cell 3 are considered in conjunction with the lateral movements of the geogrid.

LATERAL GEOGRID MOVEMENTS

Using travelling microscopes, horizontal movements of two points on the geogrid reinforcement were observed. These points were initially 1.59 m and 1.08 m from the beam centerline. The results for the initial incremental loads are presented in Figure 5. The basic movements recorded were towards the load. The first point of note is that no movement occurred prior to 8 kN of applied beam load. The second point is that little differential movement occurred between the two observed points until 25 kN of applied beam load. At this stage one expects that the geogrid will be developing tension in this outer region. This is consistent with the results given by Cell 3 and shown in Figure 4. This stage also coincides with the beginning of the separation of the reinforced from the unreinforced cases in terms of beam displacement, Figure 2. Thus one may consider that the full mobilization of all aspects of the geogrid reinforcing action are underway at this point.

The difference in movements observed between the two geogrid points can be reduced to terms of strain by considering them over a gauge length of 0.51 m. Thus at a beam load of 48 kN a differential movement of 0.16 cm would represent a strain of 0.3 percent. If

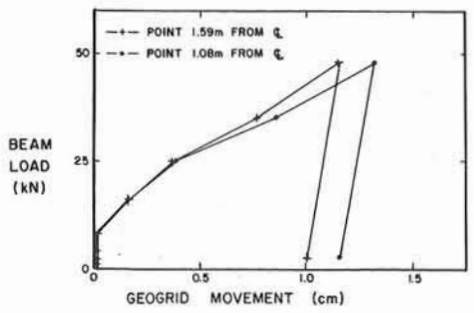

Figure 5
Lateral movements of geogrid

indeed this is a true strain in the geogrid it appears to remain "locked in" as the differential movement remained the same during the unloading cycle. This would be consistent with qualitative observations that the outer anchorage zones appear to move as a block.

Unfortunately tensile load cell 3 lay 800 mm from the centerline and the first movement gauge 1080 mm. As such they were not coincident. If one takes the liberty of assuming that they were then a combination of the two results produces an in-situ "pull-in" test or interface shear resistance test. A reasonably consistent curve of tensile load against displacement is obtained by making this assumption. If one considers the maximum tension recorded in Cell 3, 3.5 kN/m, to be pulling a block of gravel 0.305 m deep and 1.05 m long. Then this represents an average interface shear resistance of 3.33 kN/m^2 under a normal stress of 5.74 kN/m^2. The average movement of the geogrid at this stage of the test was 1.8 cm representing a mobilized shear strain of only 1.7 percent. The value of shearing resistance ties in reasonably with the vane shear resistance measured for the peat but the mobilized strain is very small compared to the usual strains necessary to produce failures in peats. It is possible therefore that greater tensions could be mobilized with greater deformations.

CONCLUSIONS

1. Tensar geogrids have been shown to have a significant effect on the bearing capacity of compacted fills over a peat subgrade.

2. Significant tensile forces were measured in the geogrid and these developed despite the very compressible nature of the peat.

3. The full spectrum of results obtained open the way for the checking and development of analytical methods and the development of a better understanding of the mechanics of geogrid reinforcement.

ACKNOWLEDGEMENTS

The author wishes to thank the Tensar Corporation for its direct sponsorship of this work and also the Department of National Defence of Canada for their continuing support.

Special thanks go to Dr. R. Douglas, now of the University of New Brunswick, who designed and built the load cells, to Mr. J. Bell who performed the testing, to Miss Martina Lahaie who typed the manuscript and Mr. J. DiPietrantonio who prepared the figures.

REFERENCES

Giroud, J.P. and Noiray, L. (1981). Geotextile-reinforced unpaved road design. PASCE, Vol. 107, No. GT9, p. 1233-1254.

Jarrett, P.M. (1983). Reinforcement of roads on organic terrain. Proc. 7th Pan American Conference on Soil Mechanics and Foundation Engineering, p. 329-342.

Sowers, G.F., Collins, S.A. and Miller, D.G. (1982). Mechanism of geotextile-aggregate support in low-cost roads. Second International Conference on Geotextiles, Vol. 2, p. 335-340.

Foundation for roads and loaded areas: report on discussion

R. J. Bridle, *Mitchell Cotts plc*

Dr P M Noss, SINTEF, Norway made an invited contribution which gave information about a field test of a road constructed in Norway during the fall of 1983.

The test section is 180m long and is based on clay. The clay is highly susceptible to changes in moisture content and it suffers a significant loss of bearing capacity during the spring/fall period.

The pavement structure consists of a wearing course of 35mm of asphalt concrete and a granular base where the thickness varies between 800mm and 400mm. Two different materials have been used as a base material - a crushed stone where a maximum size of 120mm is used, and a well-graded gravel in the second part. The test section is sub-divided into smaller sections, and on all sections a thin fabric is used as a split between the subgrade and the granular materials.

On some of the sections Tensar Geogrid SS2 has been placed on the top of the subgrade in order to study how it will affect the bearing capacity of the road. A steel mesh has been put in another of the test sections.

Sections without any reinforcement, and the section reinforced with the steel mesh, have been modelled in the inter-bed programme at the University of Illinois, and the stress model has been used to describe the elastic properties of the base and the subgrade material. Where the steel mesh has been used, computations show that we should expect a reduction of the elastic deflection beneath a 50kN single-wheeler of about 15%-35%, depending on the thickness of the crushed stone layer of the bearing capacity of the subgrade during the spring/fall. Stress-dependent moduli have to be used in these computations.

It is believed that the measured deflection and the curvature of the sections which are reinforced with Tensar Geogrid will lie between the sections with no reinforcement and the sections with steel reinforcement.

During the spring/fall period this year, elastic deflection measurements will be made at the test section. A falling-weight deflectometer simulating the moving loading post of a 50kN single-wheel load will be used in this study. By installing strain gauges in the pavement structure the mean elastic and plastic strain in the base layer can be measured, and that should give us some additional information about how compaction can affect the bearing capacity in the sections where the SS2 Geogrids are used.

The design charts presented by Dr Giroud and shown at Fig 11 of Paper 4.1 attracted a good deal of attention. Other papers were discussed in the light of the evidence they gave to support or challenge the use of the design charts for everyday engineering use.

The arguments challenging the charts cited the limited evidence available for determining, quantitively, the mechanisms through which reinforcing meshes, either elastic or visco elastic, contribute to improved performance. Pavements represent a very expensive part of the infrastructure and public authorities are risk averse. The pragmatic basis of the curves may fit observed results but extrapolation required caution. This is because their basis is not so clearly related to engineering mechanisms used by the engineering community that they generate confidence in use. In particular the method's reliance on elastic behaviour, when demonstrably it is inelastic, caused some delegates to express doubt about its use.

The argument in support of the design method was that it does not rely directly on elastic theory but rather employs elastic theory to establish direct comparison between the reinforced and unreinforced cases. This reduced any inaccuracies attributable to the use of the elastic theory. Since the charts rely on a number of variables, calibration against actual cases takes some account of non-linear behaviour through their interaction. The curves can be improved by further consideration of non-linear behaviour. They can also be improved by using them to forecast cases outside the existing experimental observations and making comparisons, that is attempting to radiate the curves. Furthermore, for most of the life of a road, induced strains would be modest. Now since existing policy in developed countries is to intervene at reasonably low levels of permanent deformation, to offset increasing vehicle operating costs, elastic analysis used on a comparative basis is probably adequate.

It was generally agreed that the curves should help engineers. Engineers can produce target designs to compare with conventional proposals on a basis of equal life. If the engineer felt the risk involved in using the reinforced design is greater than a traditional design, he can interpret it conservatively and yet achieve some of the benefits in direct cost and increased life.

There was a need expressed for the development of a design method which deals explicitly with the strength parameters of the materials involved, the variation in pavement loadings, the variation in the strength and non-linearity in the stress strain curve of the materials used.

One important variable is the elastic stiffness of granular materials. Their stiffness varies with the stress levels to which a particular element of a granular pavement base is subjected. This had been demonstrated many times in extensive testing at the University of Nottingham. The plot of elastic stiffness against initial effective stress, generally that due to over-

Polymer grid reinforcement. Thomas Telford Limited, London, 1985

burden pressure, has a very sharply curved form showing a high stiffness with high effective stress. Furthermore, good confimement will also yield high values of stiffness. However, the effect of deterioration with time, due to high repeated value of shear stress, is to reduce the stiffness to relatively low values.

If this phenomena is ignored, then the results of any design equations based upon that shortcoming will be misleading.

It is evident therefore, that increasing confinement will be an advantage because it will increase the stiffness of the base. Contributors to the discussion speculated on how this may be done. Two examples were given. Firstly, it was suggested that pre-stretching will increase confinement, or at least make its achievement more secure. Secondly, deflecting the reinforcing layer to sag below the wheel loads and hog at other places was thought by contributors to be beneficial.

Both techniques aim at enhancing the membrane effect. Pre-stretching is also aimed at increasing bond, and thereby the confinement, while profiling, will provide vertical components of the stress in the membrane, to increase the spread of load across more of the pavement.

It was doubted whether practical and economic techniques to achieve these aims can be devised. However, pre-stretching below asphalt layers is reported in papers in other sessions. Transverse deflection can be achieved by shaping a first layer of stone, returning and pulling the reinforcement horizontally over it and then pouring the second layer to stretch the membrane into the profile of the first. The description shows that the increased number of activities meant that profiling was unlikely to prove economic.

The discussion on membrane tensioning showed that more work is needed to identify the mechanism of confinement and bond. Slippage between the reinforcement and base at the higher levels of strain, or later stages of loading will have an adverse effect on performance.

Delegates were prompted to speculate on the mechanisms by which improved performance was achieved. The aim of further research should be to better identify and quantify such mechanisms, see how to enhance their beneficial effect and how to better represent them in design equations.

The discussion confirmed the basic mechanisms at work. In general an aggregate layer will deteriorate with time, due to contamination of the base by the subgrade fines moving upwards and the base aggregate moving downwards. In addition the aggregate in the base will be displaced laterally. This deterioration over time is modelled in the design method in paper 4.1 by applying different stiffness moduli for the effect of contamination and for the effect of base cracking.

The contamination can be prevented by a geotextile acting as a separating layer. However, since geotextiles are generally highly extensible, that is they induce only a little load for a large strain, it was argued that they did not contribute to confinement. Figure 9 of paper 4.1 gives the improvement due to separation as no more than 10%. In comparison containment of tensile strains by the interaction of a strong, inextensible grid with the base is attributed with an improvement of 70% even without separation. Together the improvement is enhanced to 100%.

It was acknowledged by contributors that the presence of reinforcing mechanisms is more important than separation. Nevertheless the thickness of the base and position of reinforcing layer are evidently significant variables in determining the degree of improvement due to reinforcement. It therefore surprised contributors to see that the choice of factors in Figure 9 takes no account of the ratios of material strengths of the various constituents or the thickness of the base.

Fig 9 also infers that greater benefits are achieved with time and after many repeated loadings. The inference derives from the fact that greater benefits are shown for the contribution of reinforcement to contaminated bases, and bases will contaminate more with time and loading. However, at higher strains and many repeated loads, the assumption of continuing quality of confinement might be doubted since the effect of migration of fines and repetition of load might affect bond. In the papers the expression of improvement in performance is taken to be an increase in the angle α, the angle of spread from the load through the base. That is, it is assumed that the pressure on the subgrade is more widely distributed, just as though the base is thickened. The adoption of such a concept stems directly from static considerations. In reality the problem is one of repeated loads and the aim of design is to maintain some restraint on the accumulation of permanent deformation.

However, the majority of discussion concentrated on the contribution each of the three mechanisms makes to the angle α rather than their contribution, under repeated loading, to restraining the accumulation of permanent deformation.

Many considered that the tensioned membrane effect makes no significant contribution because, in static terms, it is evident that the membrane load needs to be deflected to provide a vertical contribution to load carrying. The Chairman noted that if the membrane is loaded, it absorbs energy and thereby must help to reduce cumulative deflection.

It was agreed that the effect of confinement in strengthening the load carrying capacity of the base, particularly at loads which will otherwise induce large tensile cracks, is a significant mechanism in improving load carrying capacity. In addition, subgrade materials are damaged by movement at the interface and Geogrids helped restrain such movement.

The design method adopted in paper 4.1 does take account of these advantages by a reduction of strength in the unreinforced case. It was also observed that the findings recorded in paper 4.2 show an over prediction of bearing capacity for the unreinforced case if such softening is not considered.

There was a measure of agreement between authors of papers 4.1 and 4.2 about the equivalent angle α and its improvement due to the mechanisms described. For small strains, induced under static loading, it is generally expected that the effect of reinforcement spreading load to the subgrade would be small. However, for larger strains, it seems that the reinforcement makes a much greater contribution to load spreading. As time passes or more axle passes are experienced the angle α reduces in both the reinforced and unreinforced cases due to increased contamination.

In summary, the Chairman concluded that more work is needed to establish how the mechanisms worked in

improving performance. He suggested that improved performance for the road engineer is not the change in the angle α but rather that the residual deflection under each load pass is reduced. He believed that if the approach to the mechanisms is to establish their contribution to dynamic rather than static performance, engineers will increase their application of reinforcing techniques. Engineers are inherently conservative. Large economic losses result from poor prediction of performance in the design of civil works and premature failure of road pavements has already induced a high degree of political sensitivity.

Increase in bearing capacity in the case of foundations, and increase in the life of pavements, are not radically different problems. However, they are dissimilar in the nature of the loading and the criteria in respect of limit states. They therefore require separate design methods. Some departure from the traditional methods for designing roads based on load spreading seem warranted. In addition, road design needs to allow explicity for the great variations in strength due to materials and workmanship in use in construction.

The key question is "What percentage of failures before design life is complete are clients prepared to accept?"

It is evidently very small and therefore high percentile values of material strengths need to be adopted and used in designing pavements.

The Chairman thanked all authors and contributors for a thought provoking Session which had contributed significantly to the general understanding of the behaviour of pavements with Geogrids.

Participants: Dr Bonaparte

Dr Giroud

Dr Milligan

Mr Wood

Professor Brown

Mr Bridle

Mr Knutson

Foundation for roads and loaded areas: written discussion contribution

B. J. Robinson, Cheshire County Council

I would like to comment on the use of Tensar SS1 geogrid on the A51 Tarvin SW by-pass. A length of carriageway 315 m in shallow cutting comprised of silty, sandy clay had a very low CBR. A decision was made to strengthen the subgrade using two layers of SS1 with 600 mm thick 75 mm down crusher-run limestone. Over a section of 120 m the subgrade was very soft and wet and a layer of Terram 1000 fabric was placed below the bottom layer of geogrid to prevent the ingress of the wet fines into the rock layer.

The crusher-run material delivered to site was 100 mm down which proved to be too coarse and resulted in the geogrid mesh being cut in places. However, the overall result was successful and plate bearing tests were done on the top of the rock layer and also on top of the overlying sub-base which was 150 mm thick type 1 to the DTp specification. Table 1 shows the equivalent CBR results which were obtained. The recommended minimum CBR value on the sub-base is 30 and this value was easily achieved with the exception of one result in the very soft area.

Table 1. Equivalent CBR values

Chainage	CBR on rock layer	CBR on sub-base
770 E/B	40	70
850 W/B	44	>75
910 W/B	30	50*
923 E/B	12	33*
938 CL	36	48*

* Area includes use of geotextiles